Space Weather in Morocco

Pr, Aziza Bounhir

Faculty of Sciences at Rabat, University Mohammed V

How we get involved in space weather research

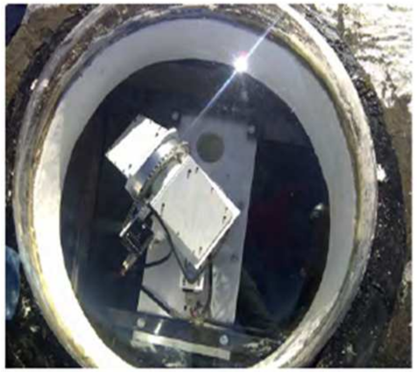

- In 2010 an ISWI delegation arrived to Morocco with proposed installations of observation instruments.

- In November 2013, the RENOIR "Remote Equatorial Nighttime Observatory of Ionospheric Region" experiment in collaboration with the University of Illinois has been depoyed at Oukaimeden Observatory.

- In May 2014, International School on Space Weather at Cady Ayyad University.

Impacts of space weather events

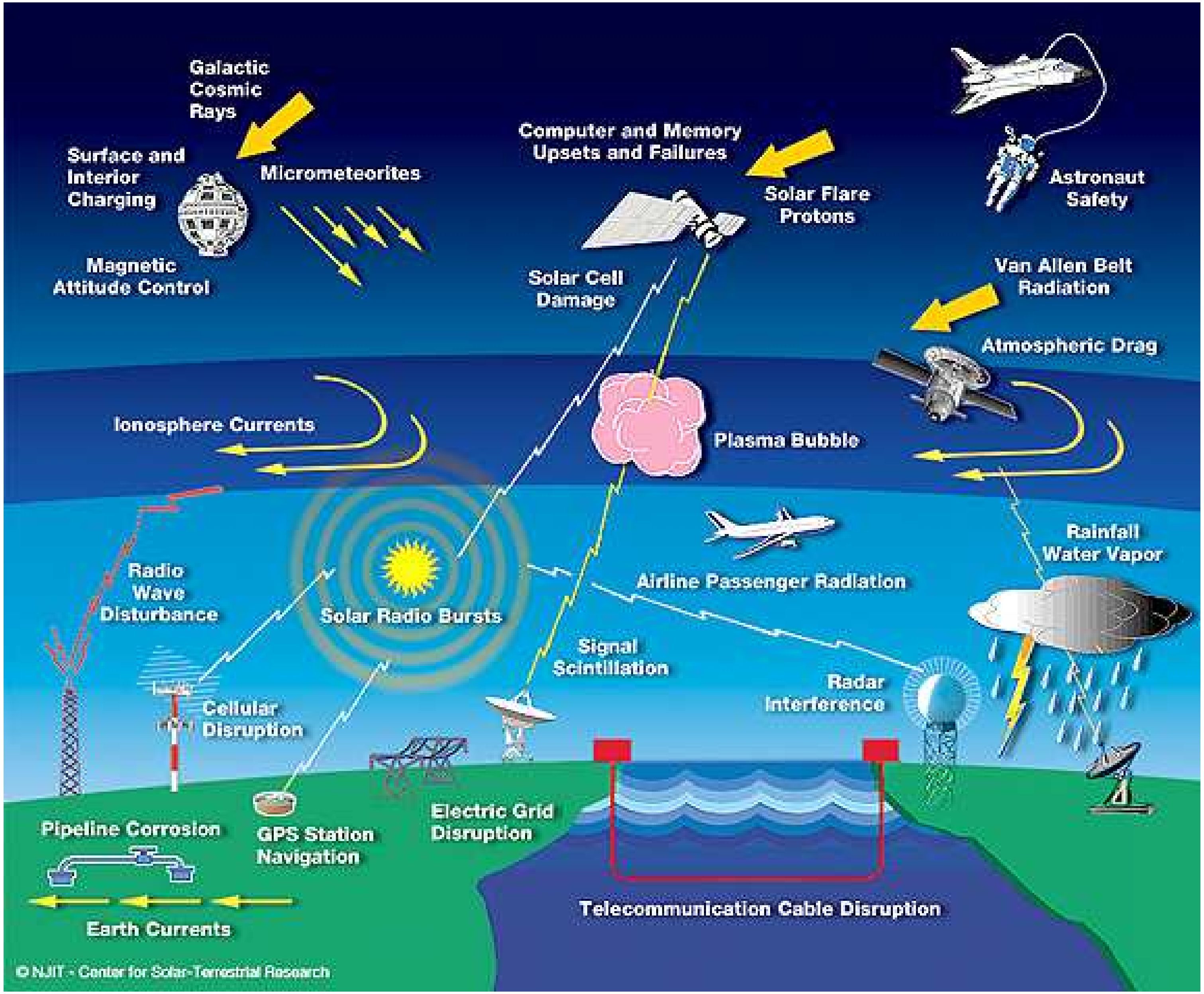

Fabry-Perot interferometer

- Light enters two parallel, partially-reflective glass plates after passing through the redline filter and is then focused onto a CCD
- Plate separation causes phase offsets that create interference on the imaging plane

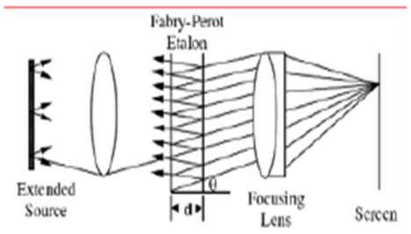

- Fit fringes to model and back out relevant airglow parameters through an inversion

- Background ~ I_B
- Intensity ~ I_0 - I_B
- Velocity ~ $\Delta\lambda_0$
- Temperature ~ σ_{FWHM}

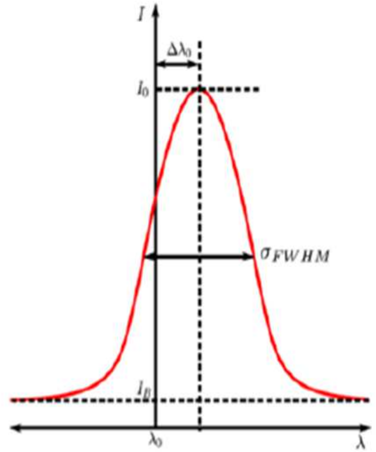

Oukaimeden Observatory (31.206◦N, 7.866◦W, 22.84◦N magnetic)

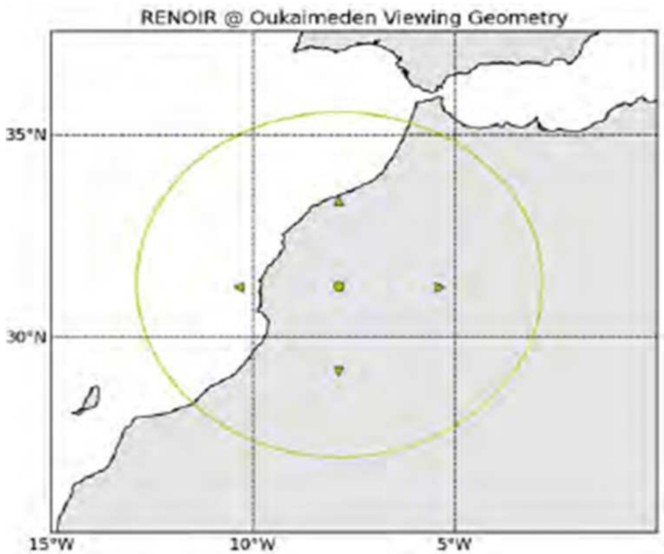

Picasso Camera

Ionospheric imager
– Measures 630.0- and 777.4-nm emission plus background
– Visualize two dimensional structure of phenomenaJ

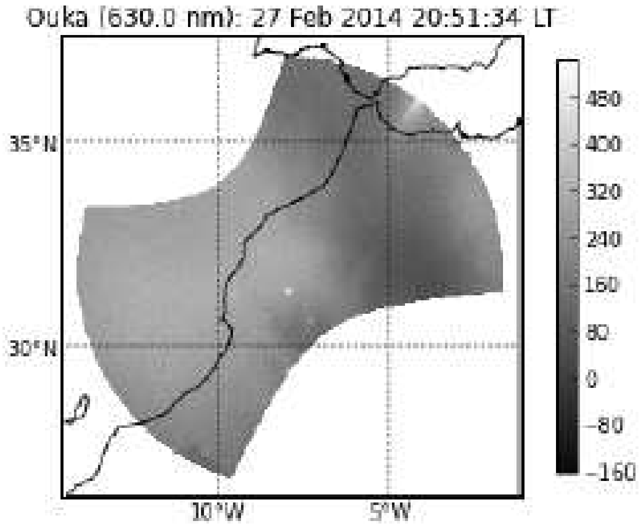

<u>Visible phenomena that can be captured</u> :
-- Equatorial Plasma Bubble (EPB)
– Medium-Scale Traveling Ionospheric Disturbance (MSTID)
– Gravity Waves
– Brightness WavesJ

Stations GPS au Maroc

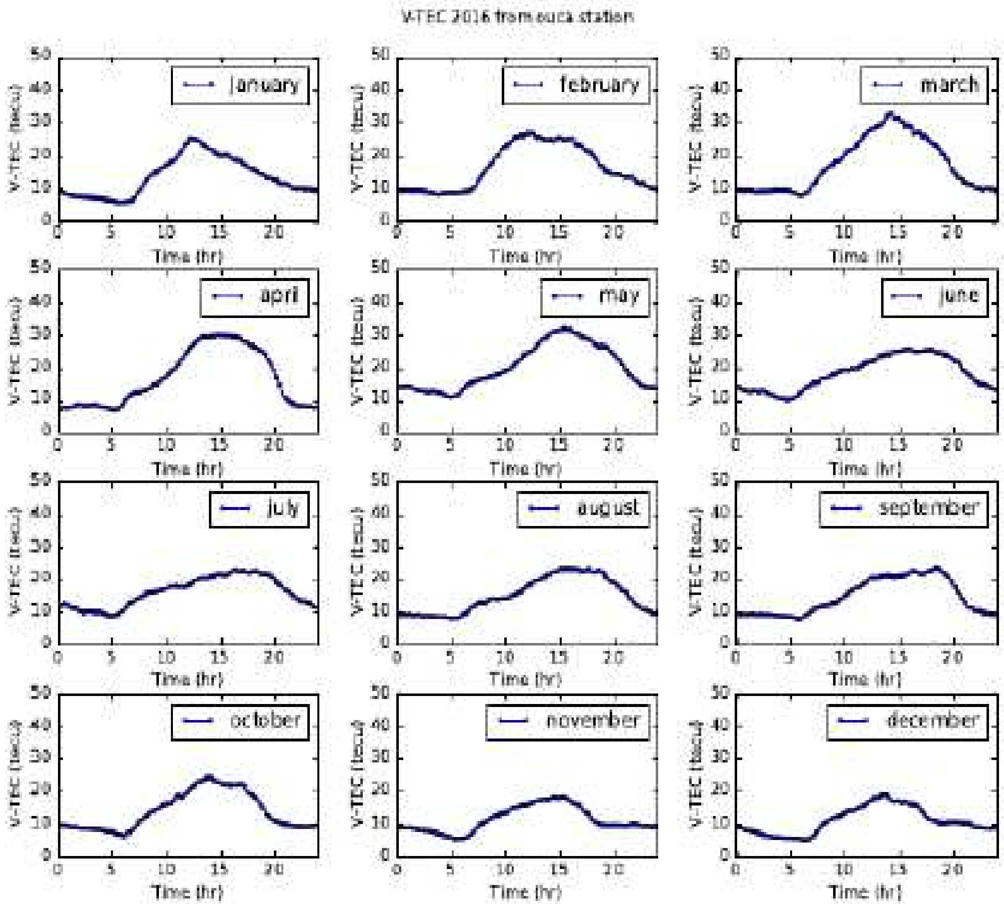

FIGURE 1.3 – La moyenne mensuelle de la station OUCA pour 2016.

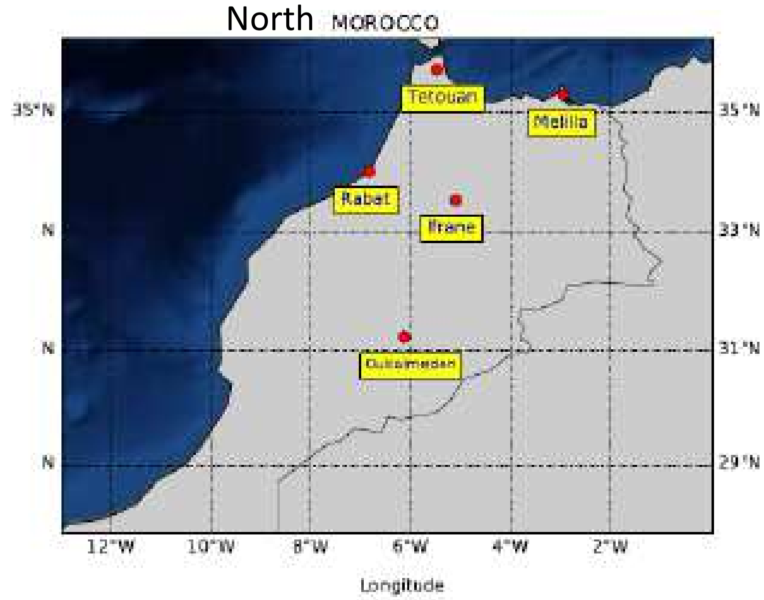

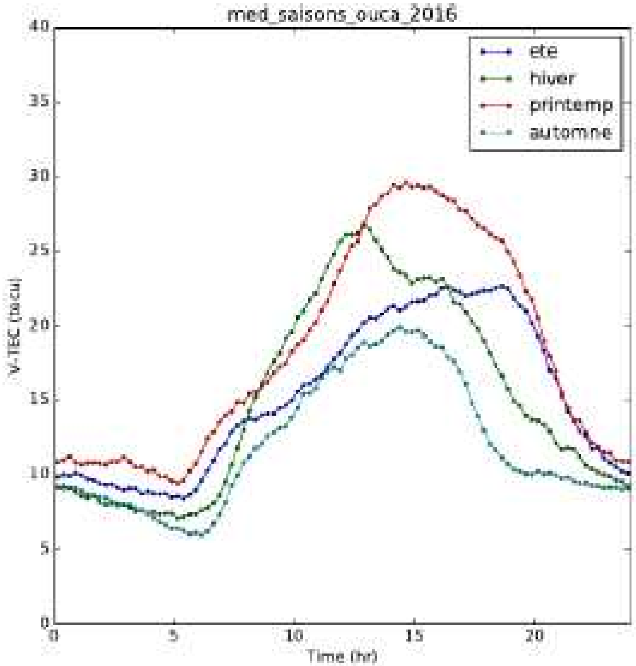

Stations GPS au Maroc

Storm times

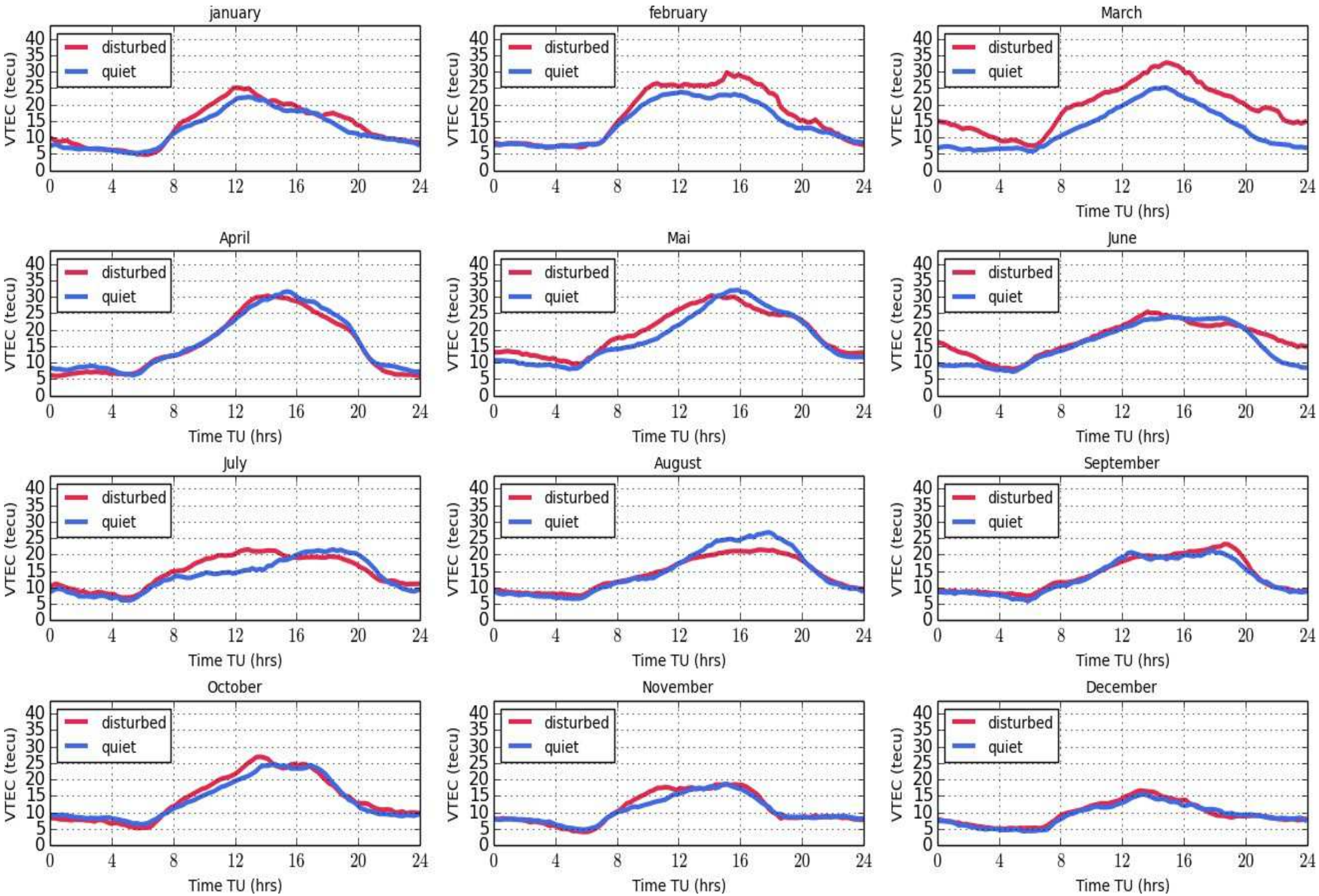

Stations GPS au Maroc

Storm times

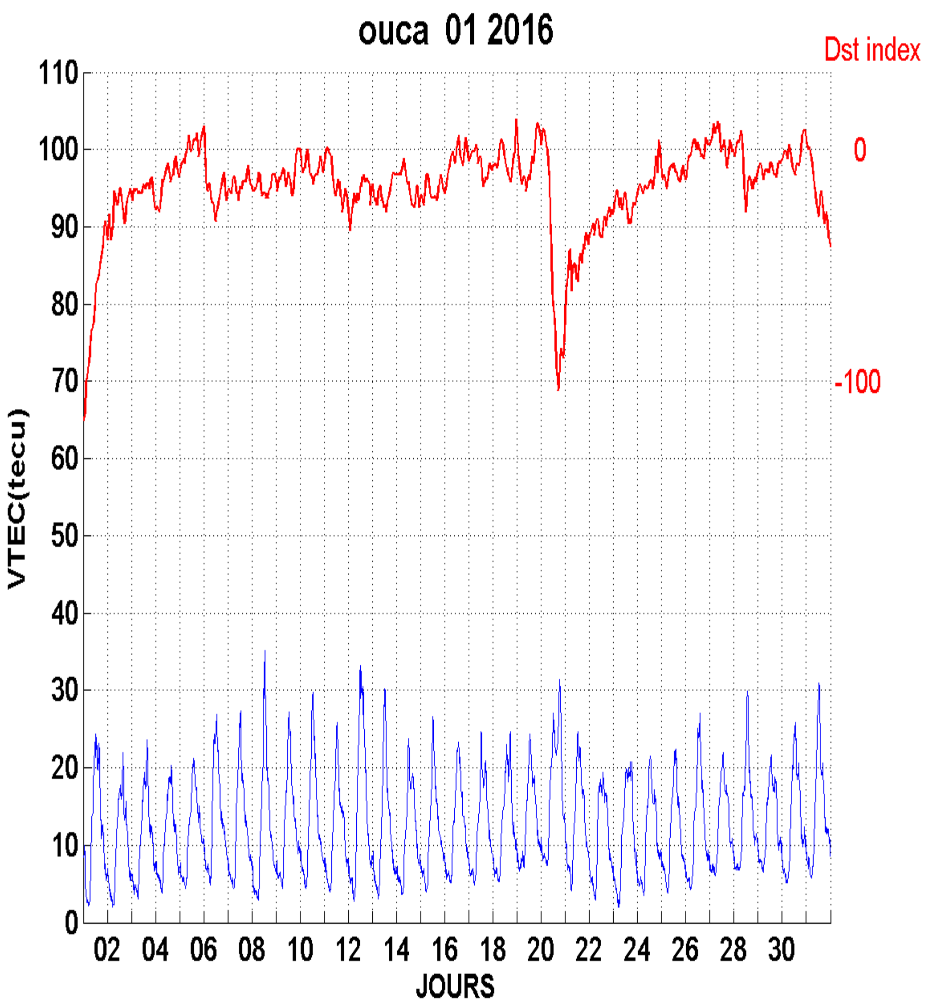

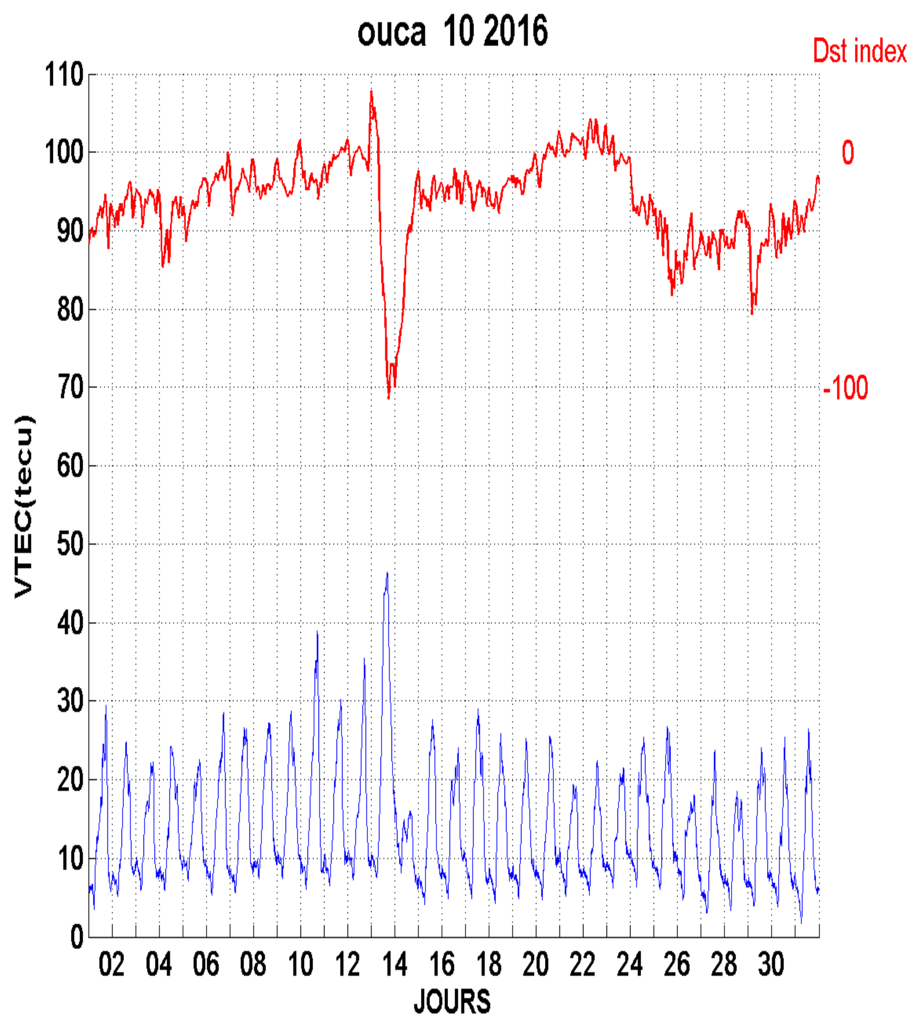

Scientific objectives and acheivements

RENOIR experiment at Oukaimeden Obesrvatory: FPI et Camera

- Measurement of **winds**, **temperature** and **ionospheric irregularities** at 250 km of altitude.

- Thermospheric winds and temperature establishement; Climatology, saisonality, solar cycle dependence, effect of geomagnetic storm …
- Tidal and gravity wave signatures
- Climatologies of EPBs over Africa
- Response of the thermosphere to geomagnetic storms.

Other data and facilities

* Meaurements of **TEC** : GPS station at Oukaimeden, and other stations in Moroco
* Make use of **satellite data, SWARM**.
* **Comparison to empirical and physics based models :** HWM14, NRLMSIS-00, TIE-GCM and GITM

RENOIR Network

- Complements observations made by similar equipements in other locations.
- Four FPIs installed in Ethiopia, Nigeria, Ivory Coast and South Africa allowing comparisons within Africa for the first time.
- Allows for studying latitudinal and longitudinal effects and differences for various phenomena
- Increased coverage to understand storm-time response.
- Wind signature related to ionospheric irregularities.
- Added coincident data from satellite observations and GPS measurements.

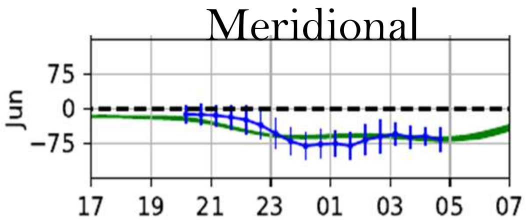

Very Quiet time wind patte

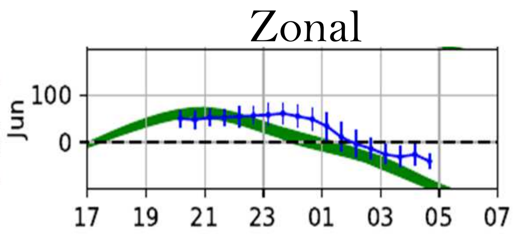

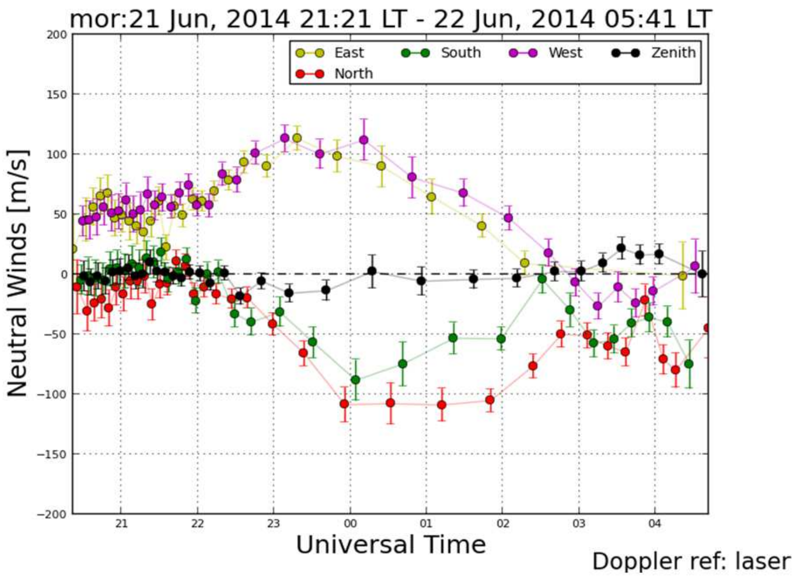

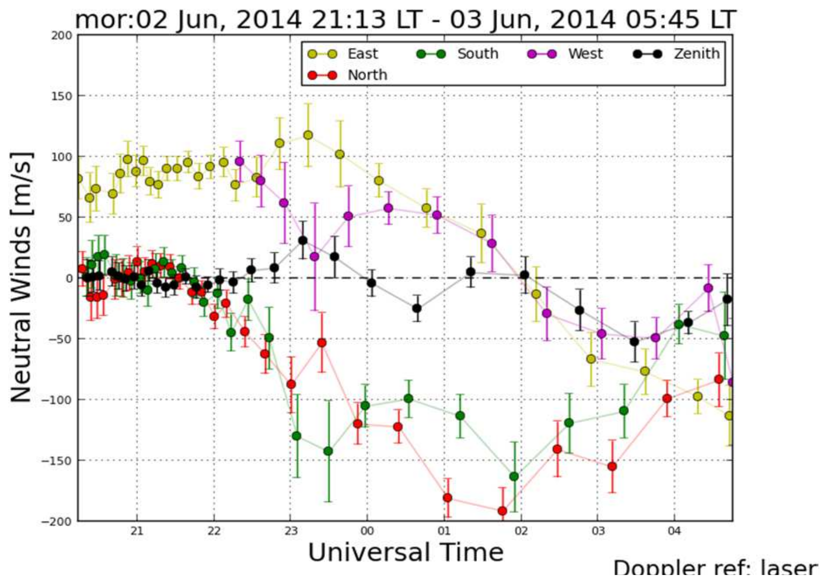

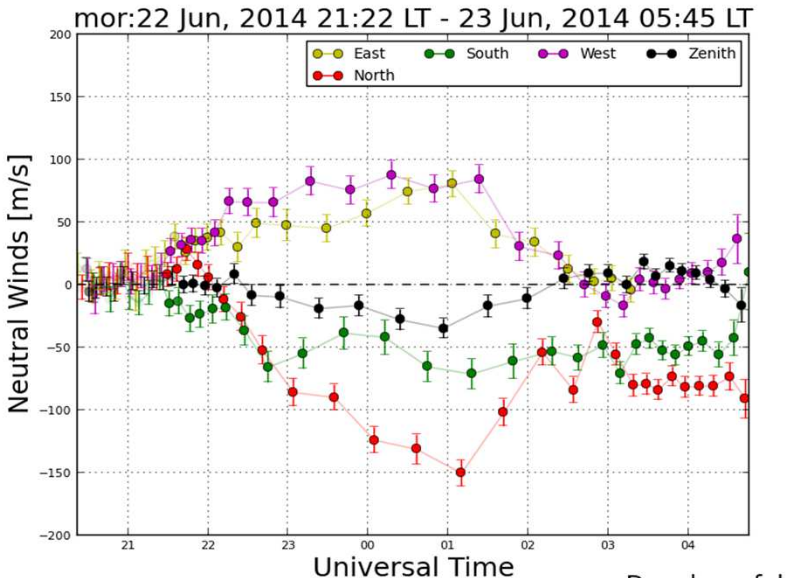

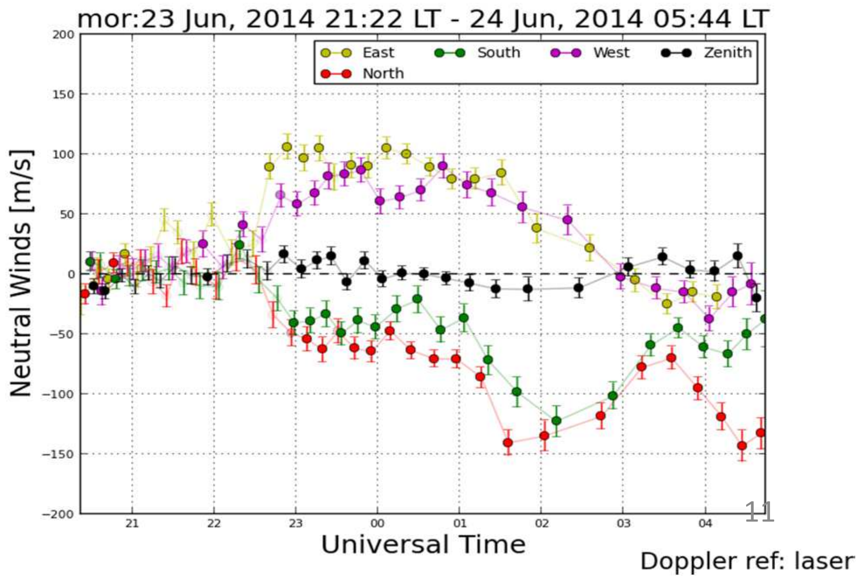

Climatology of the meridional winds

Comparison with HWM14 model

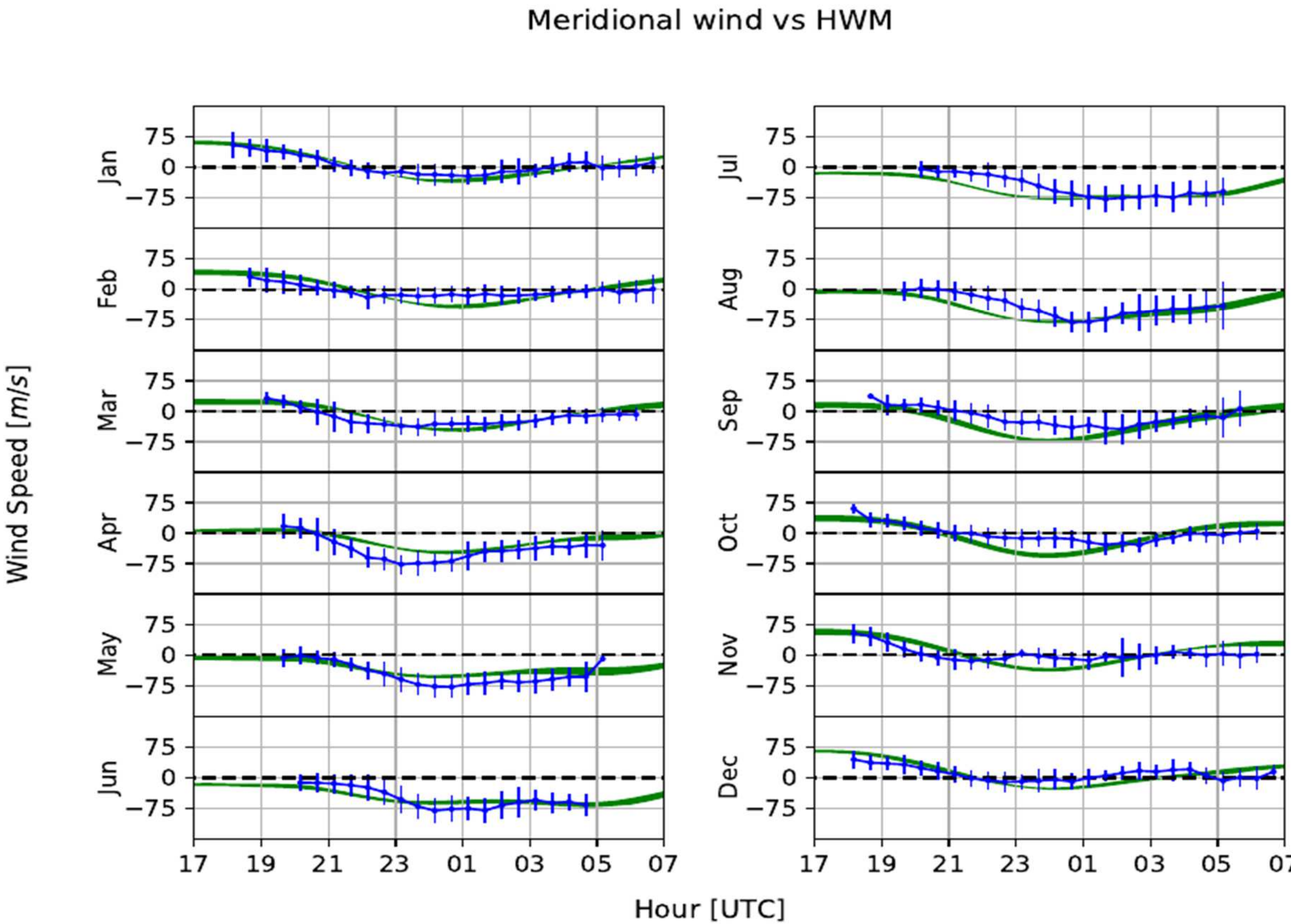

Climatology of the zonal winds

Comparison with HWM14 model

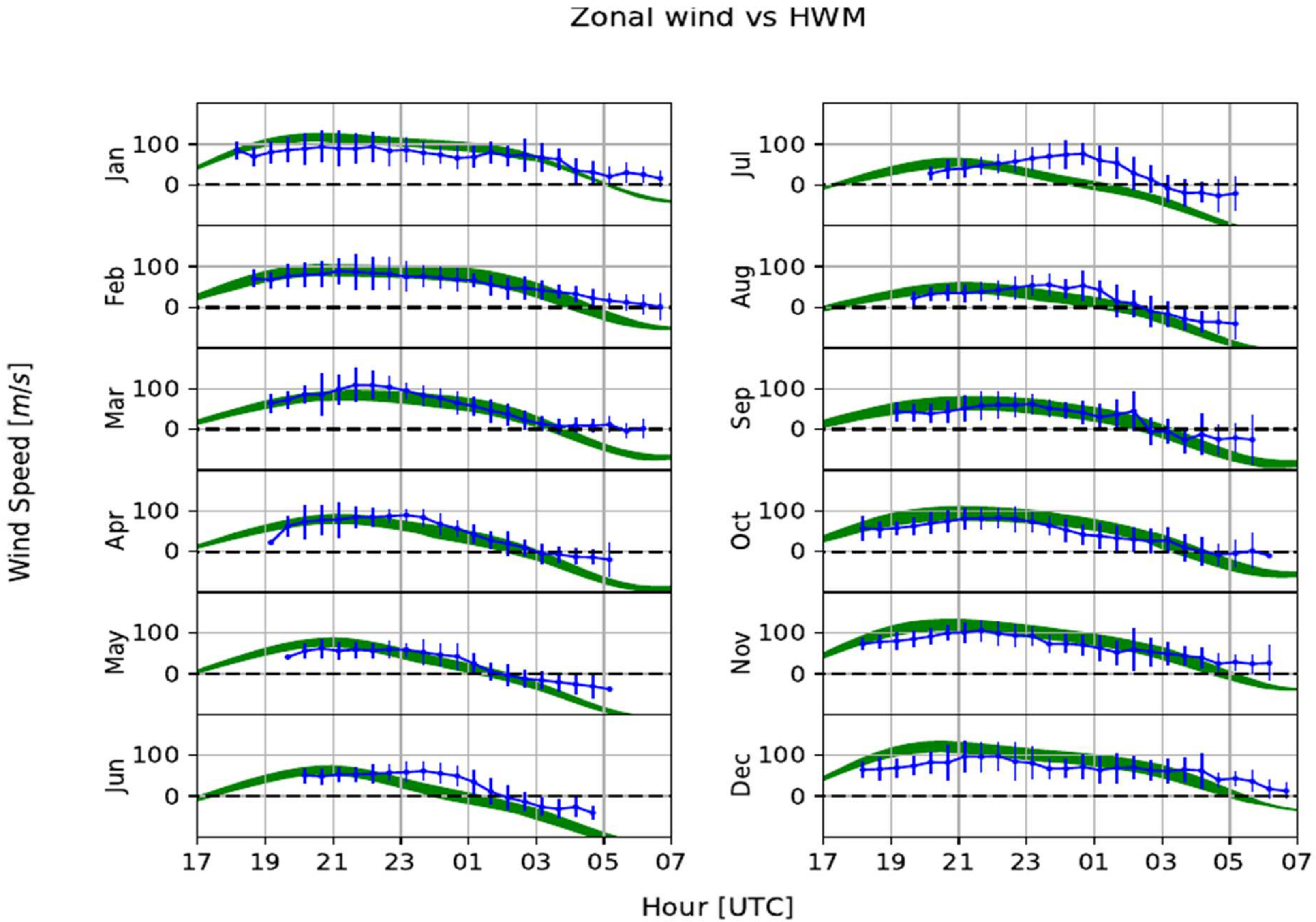

Variability with saisons; Meridional and zonal Winds

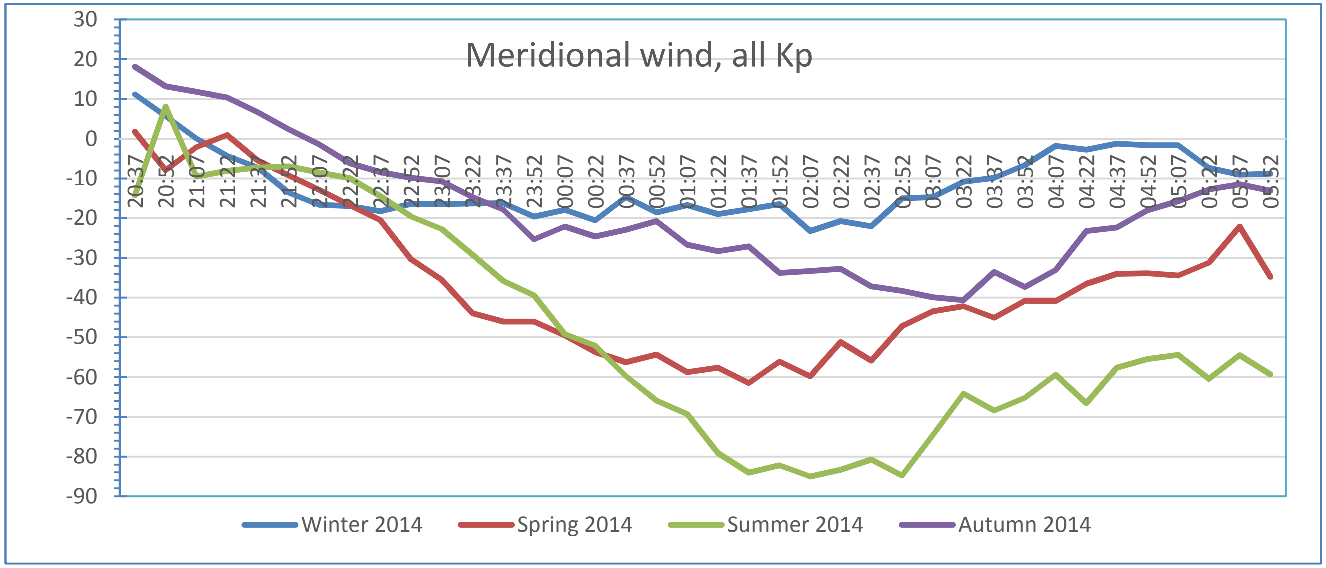

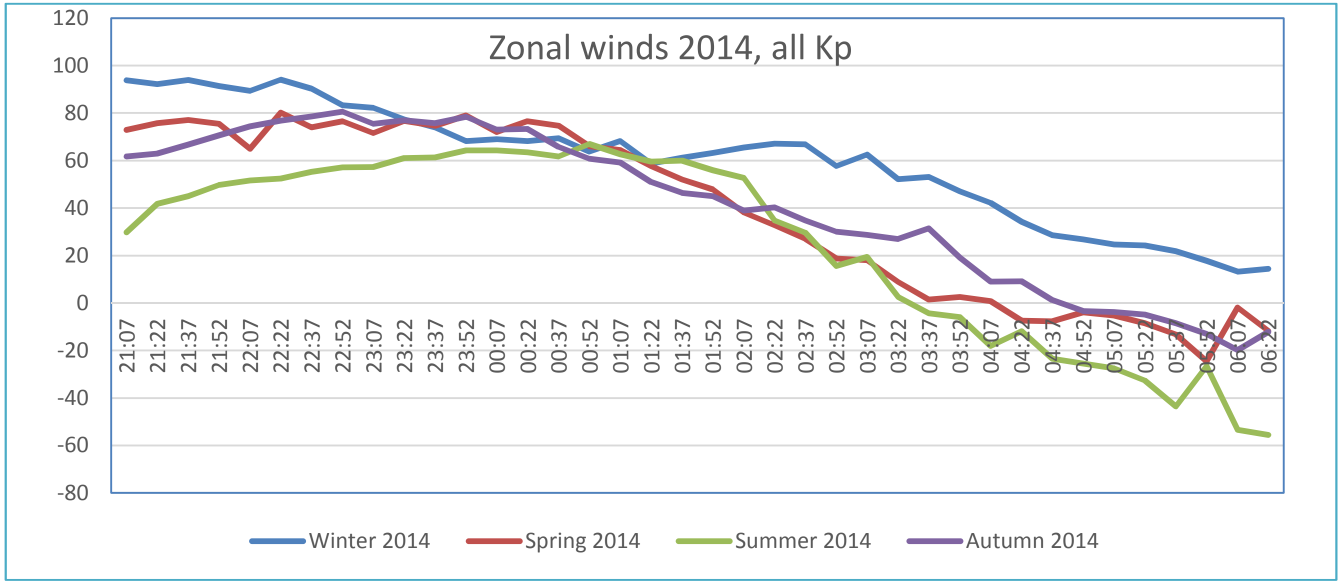

Variability with saisons; Temperature

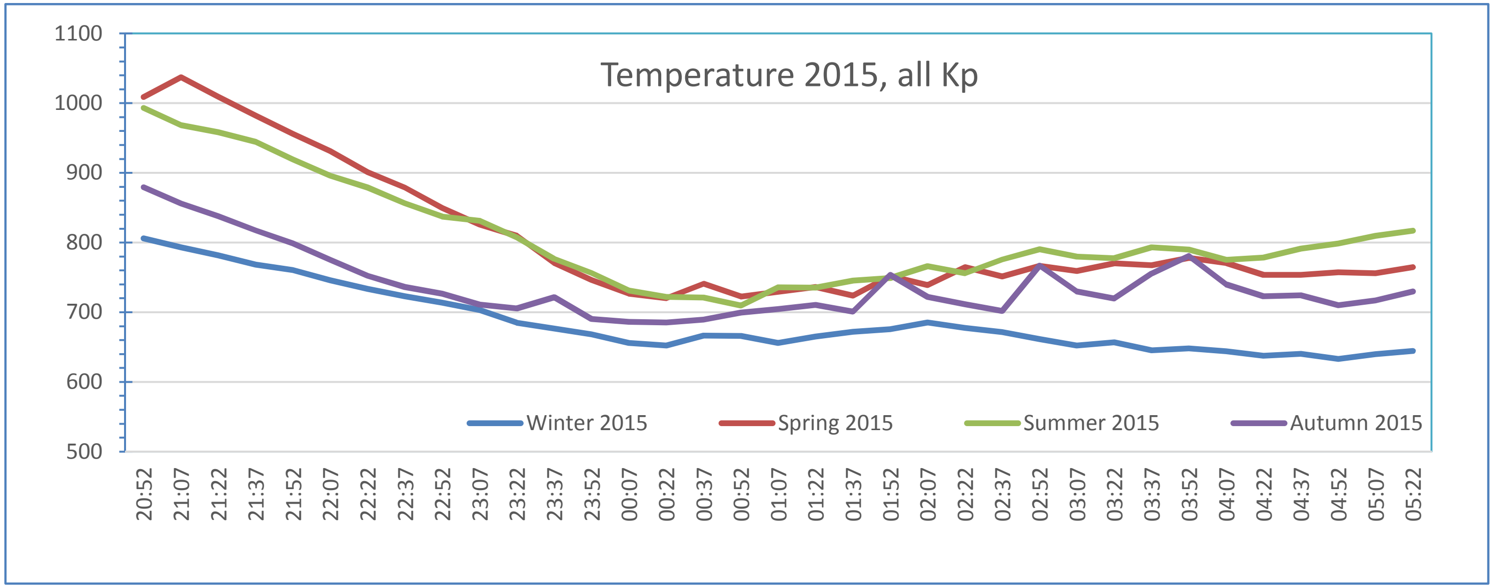

Variability with saisons; Vertical Wind

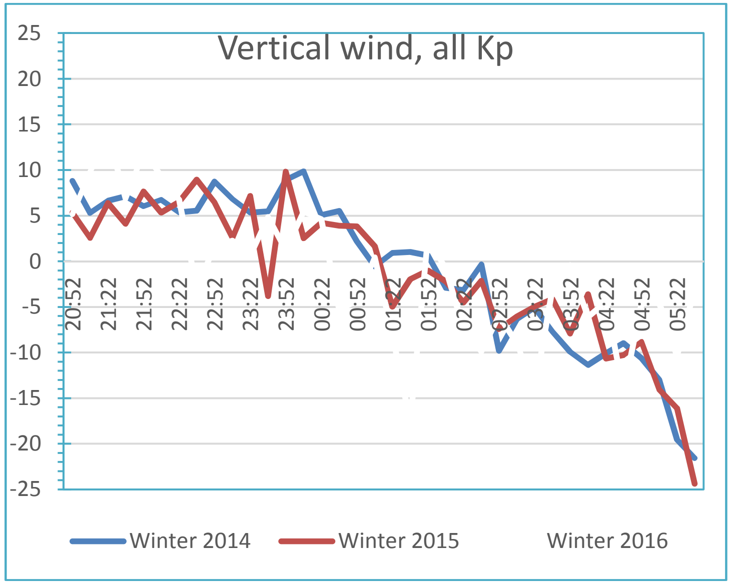

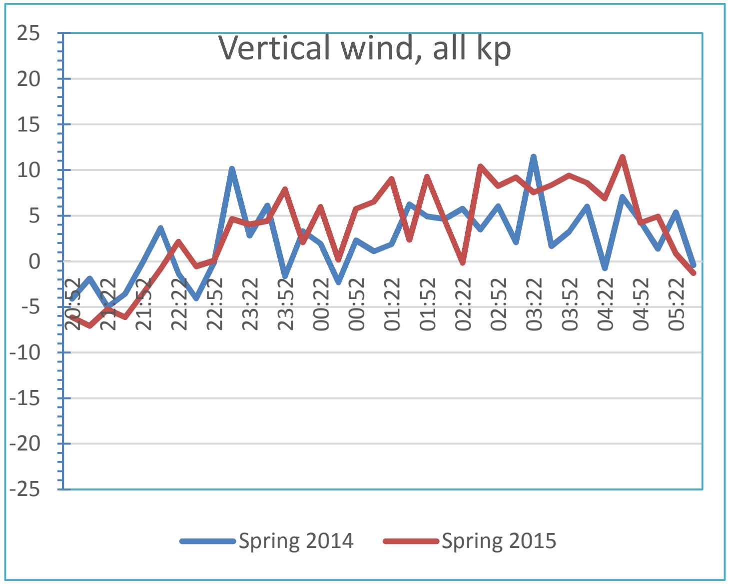

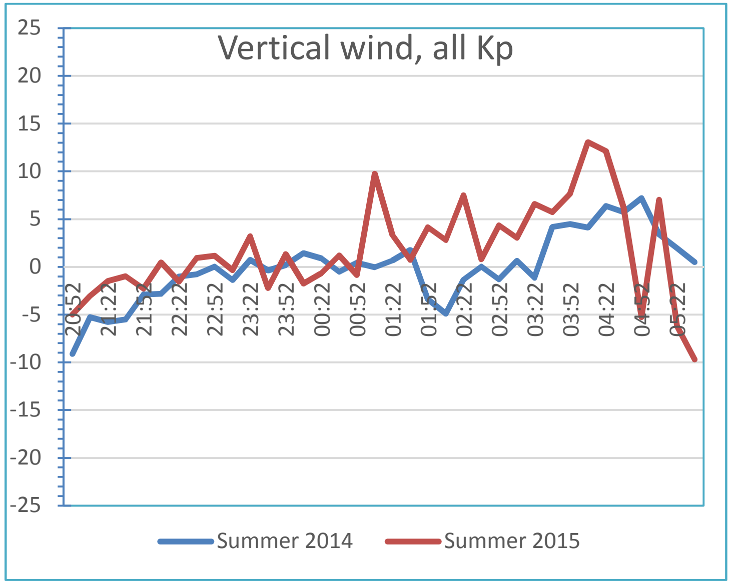

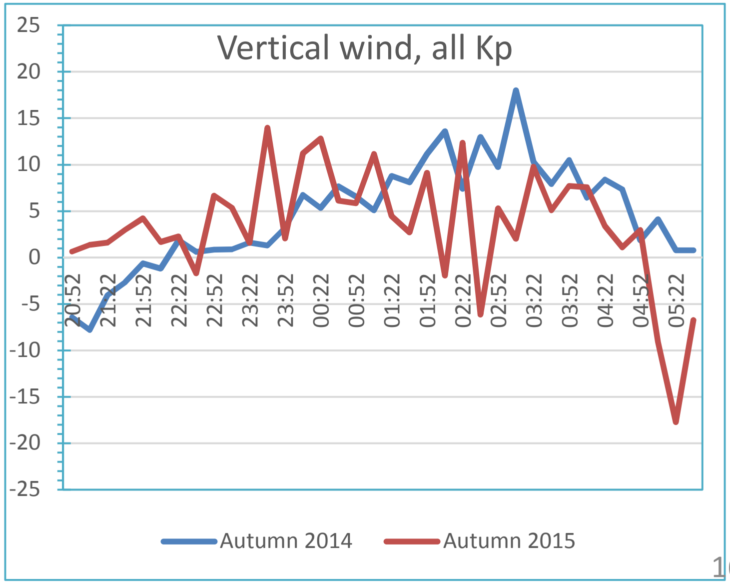

Variability with the solar cycle; Meridional wind

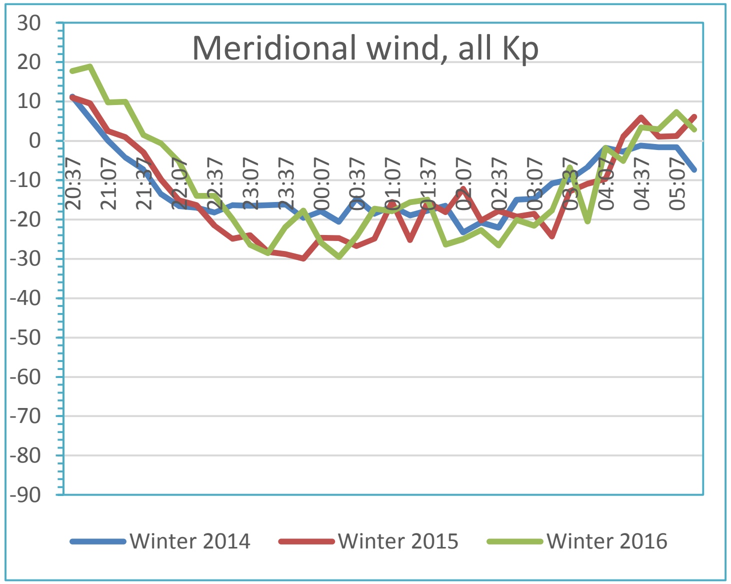

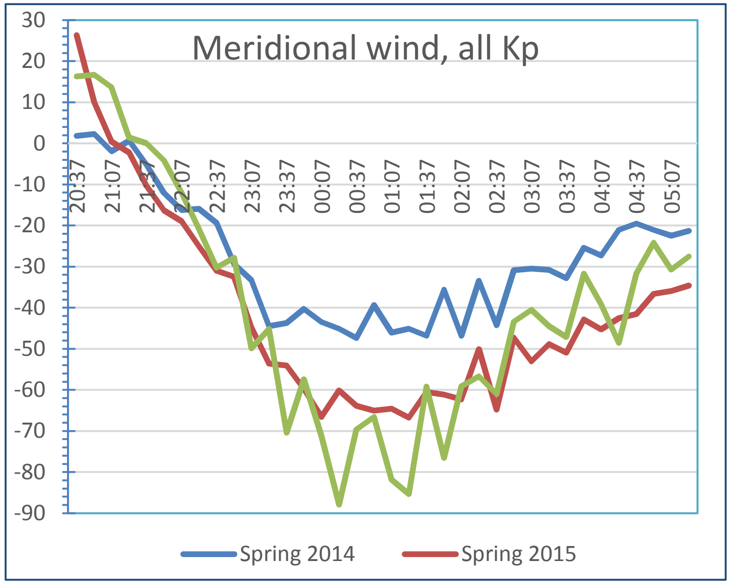

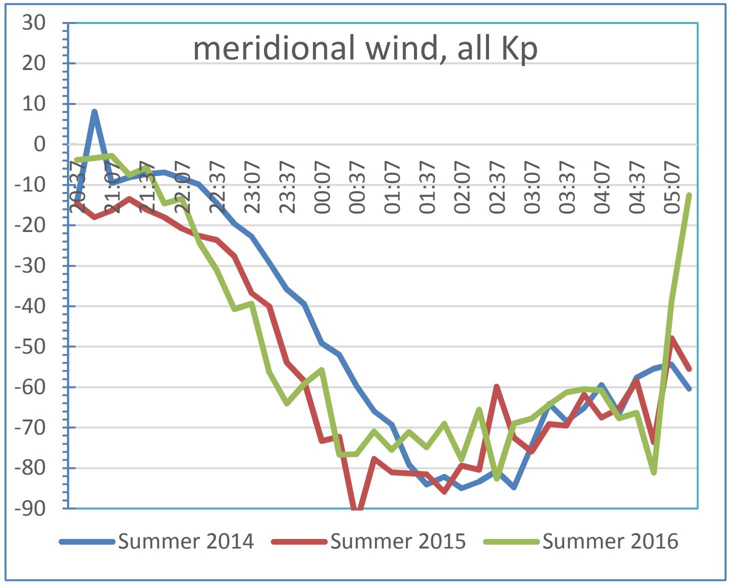

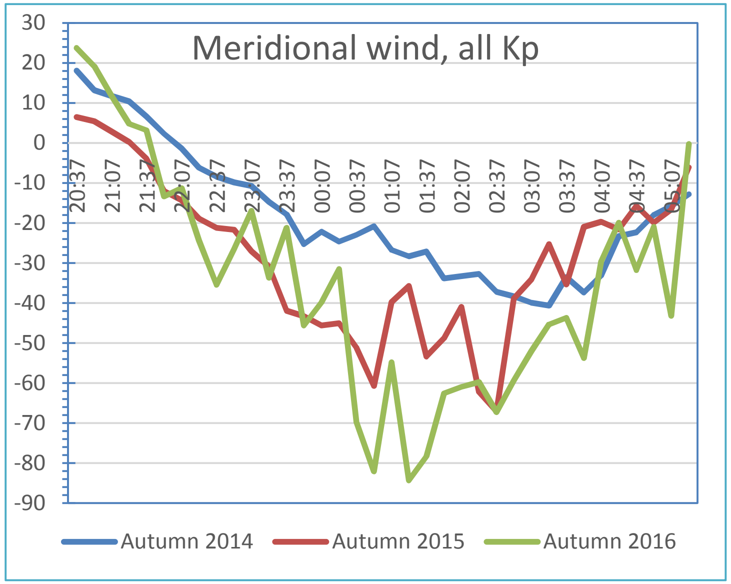

Variability with the solar cycle; Zonal wind

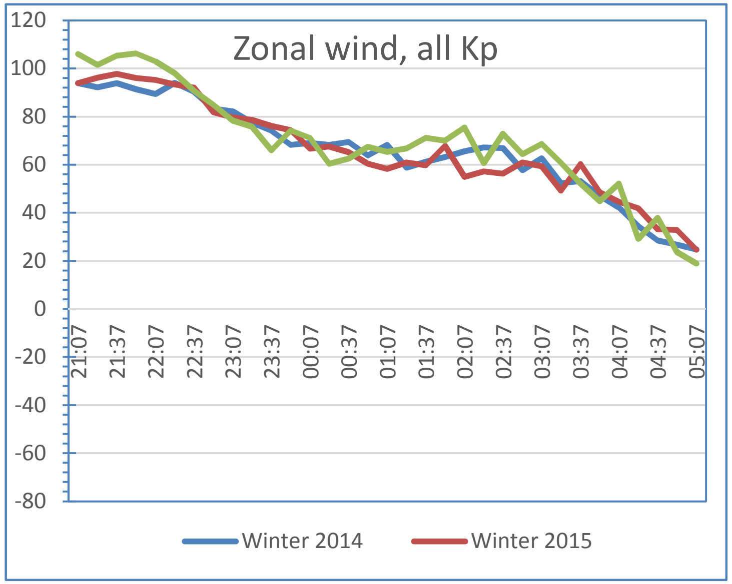

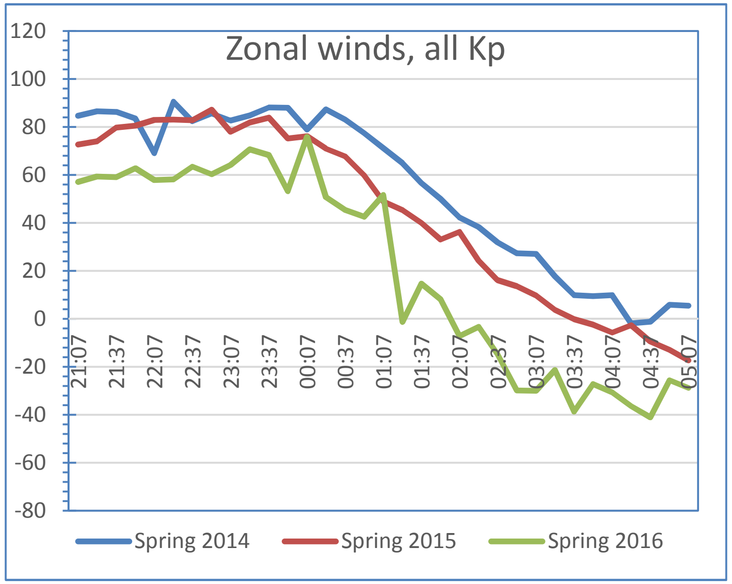

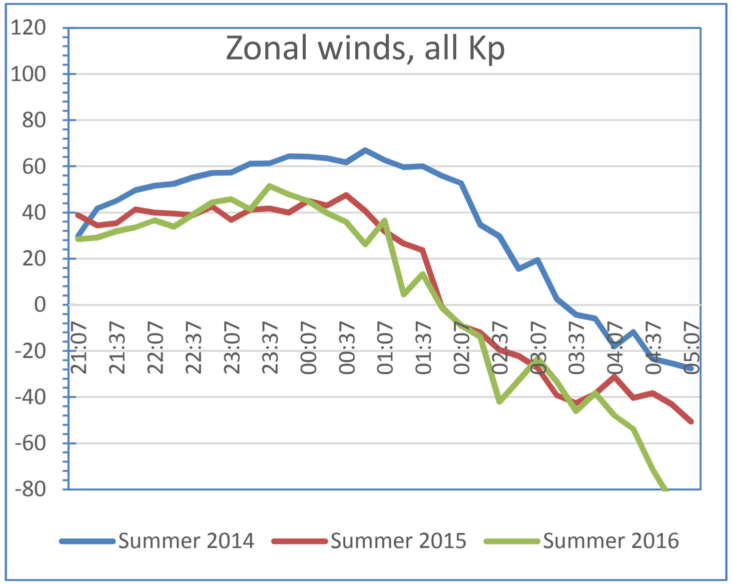

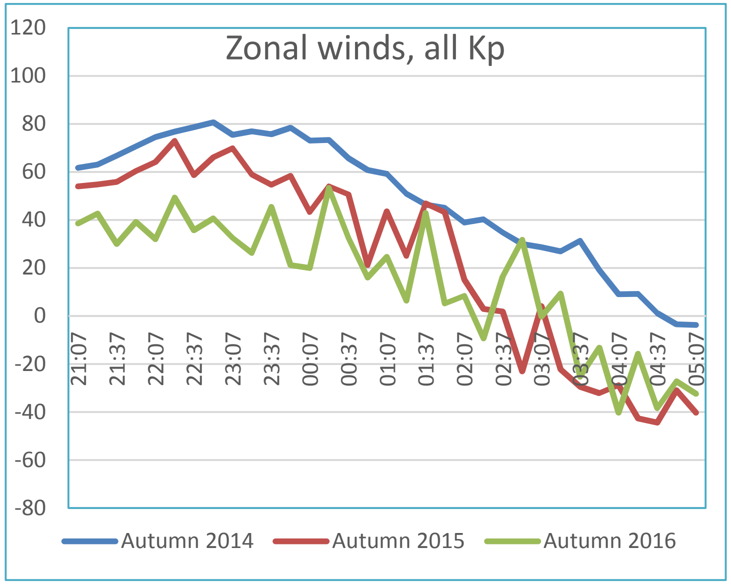

Saisonal variability with the solar cycle

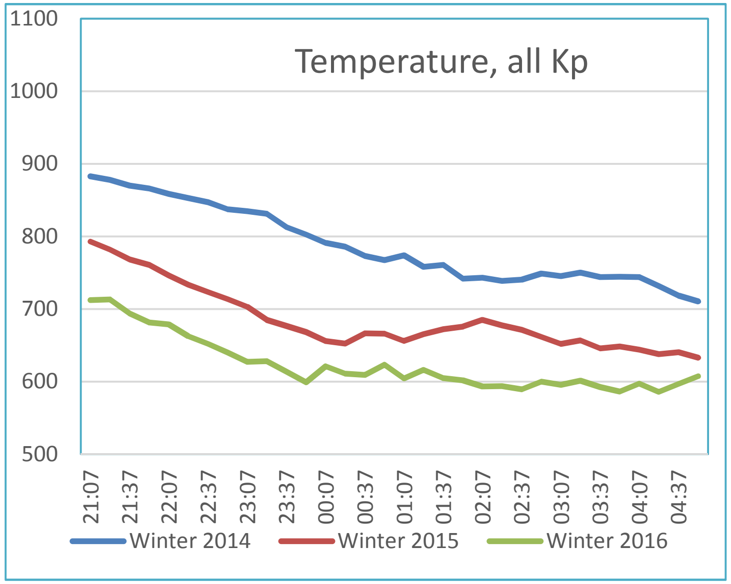

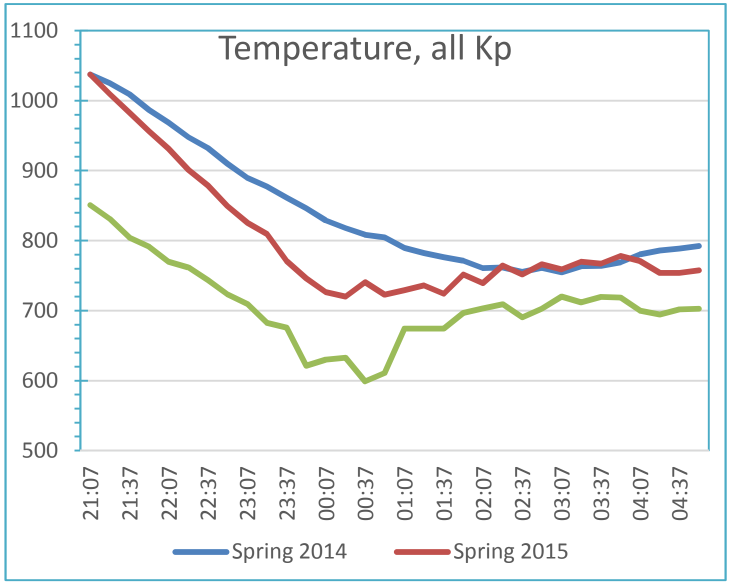

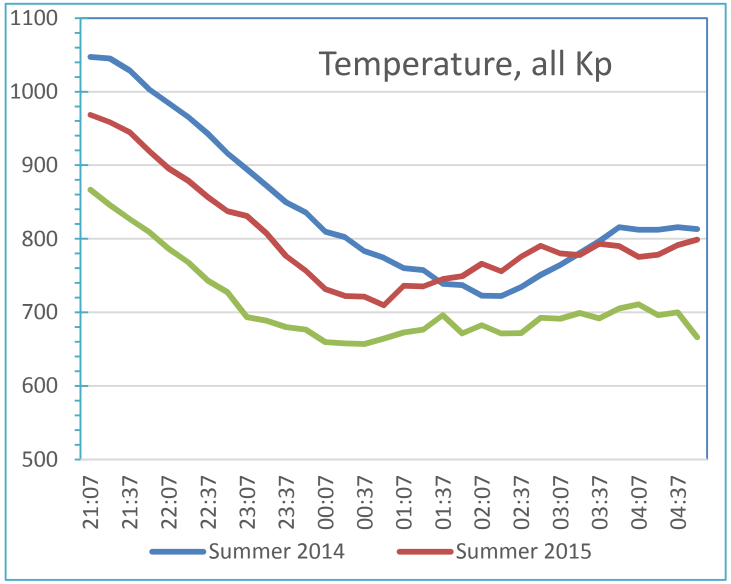

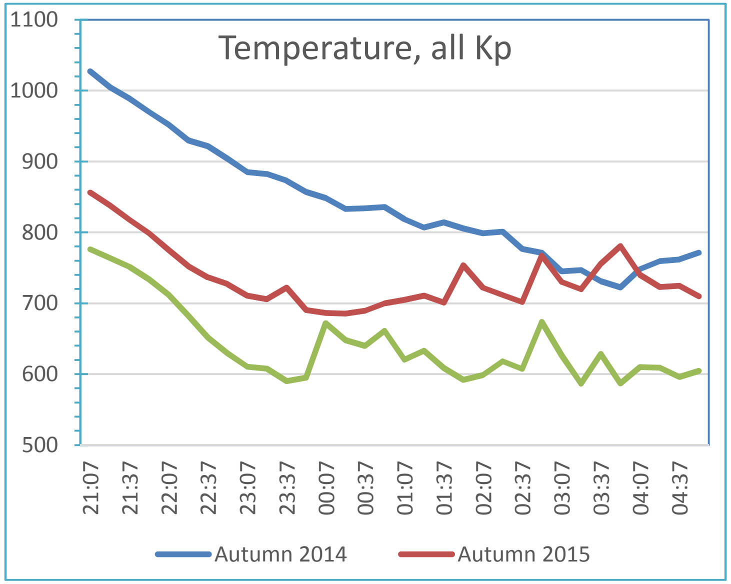

Quiet and Storm time

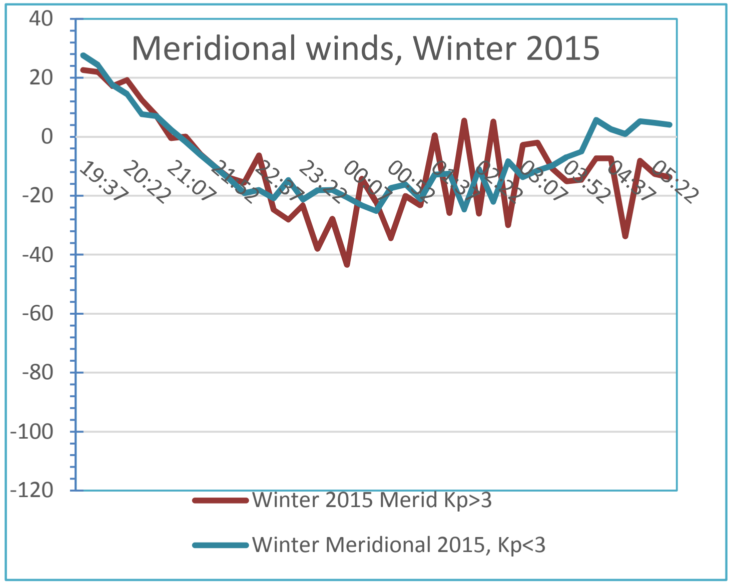

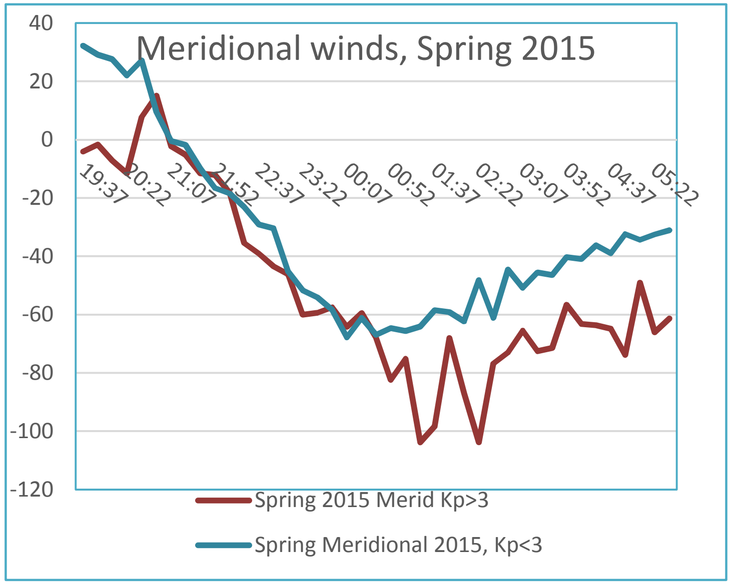

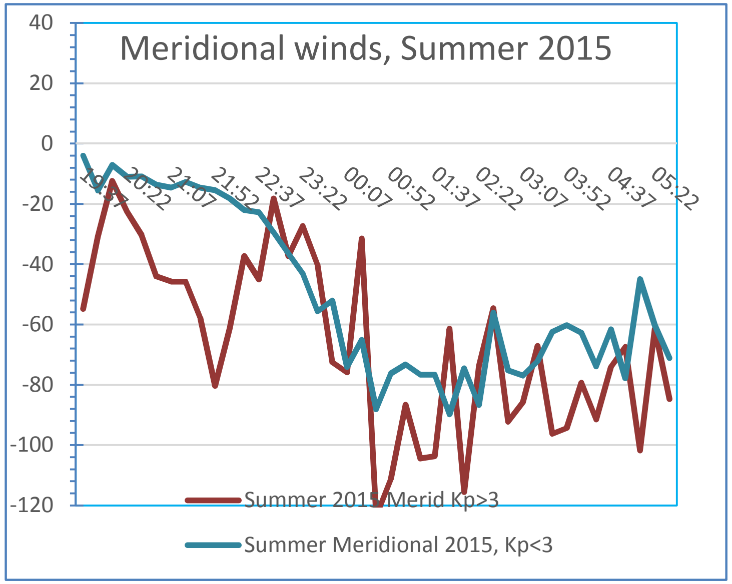

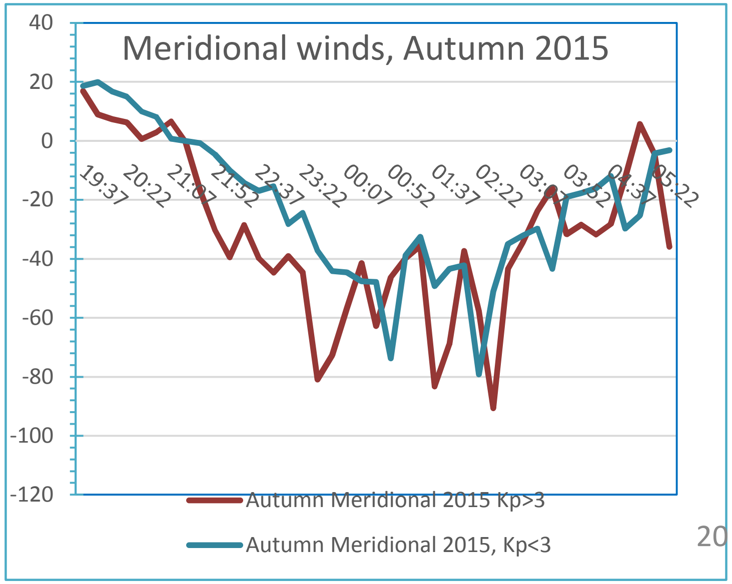

Quiet and Storm time

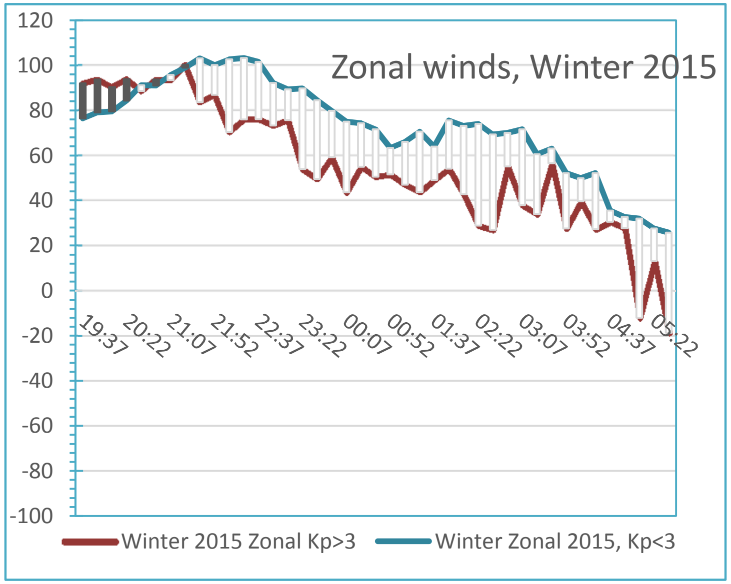

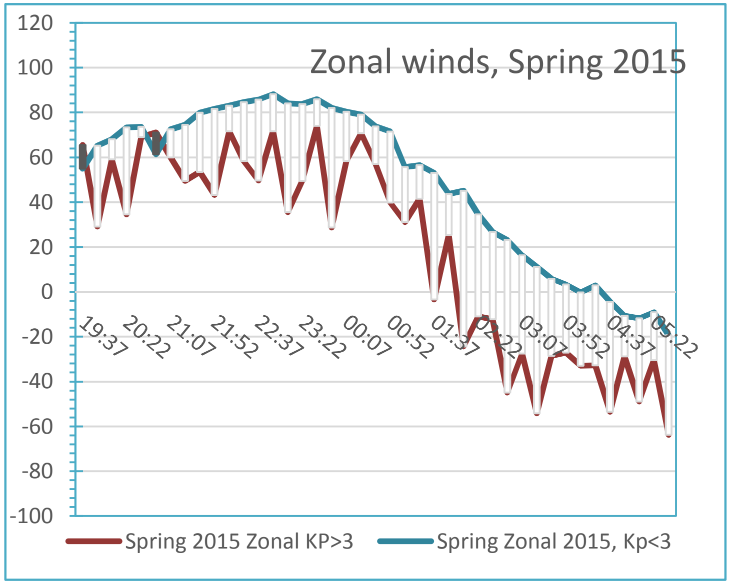

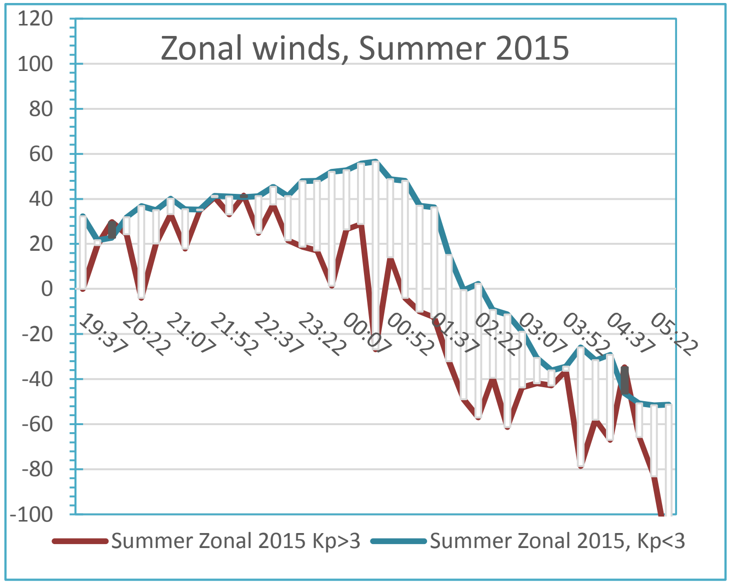

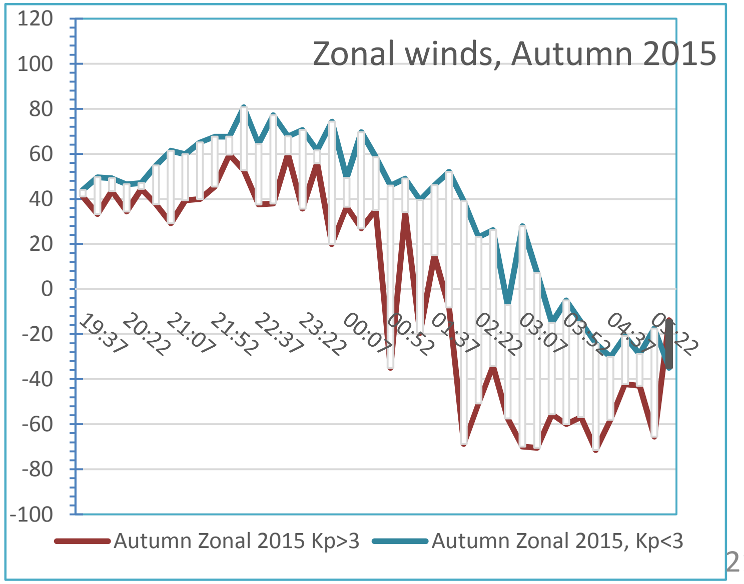

Quiet and Storm time

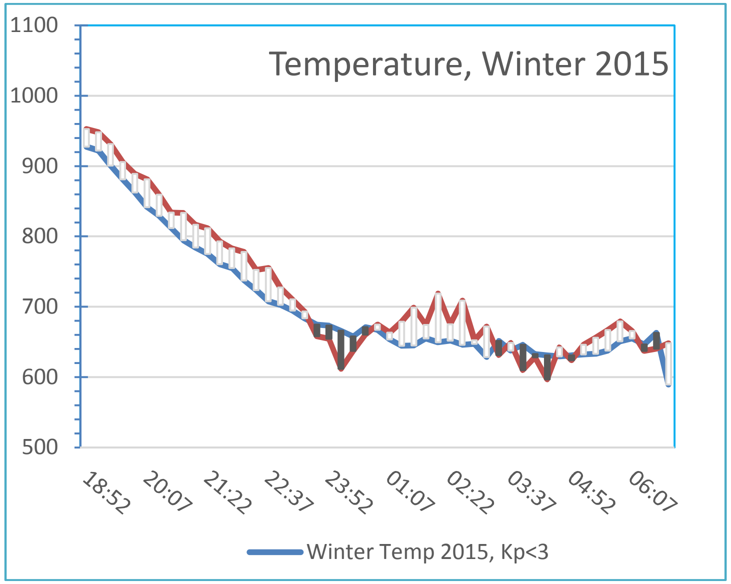

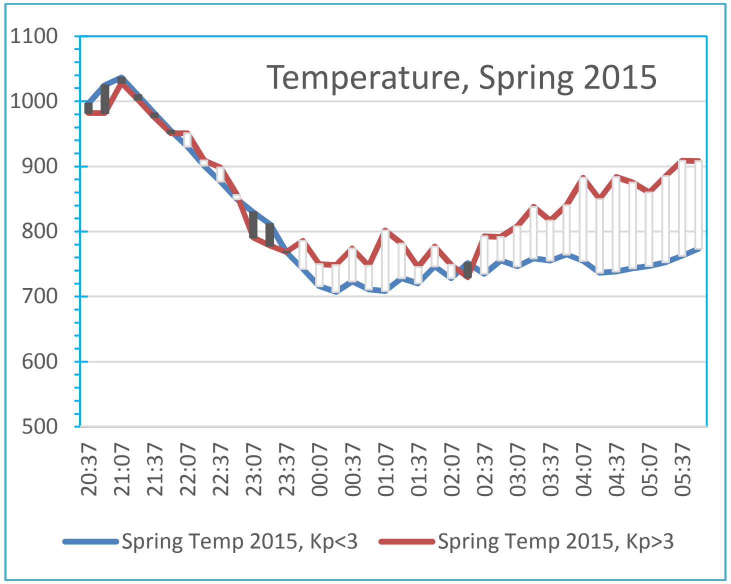

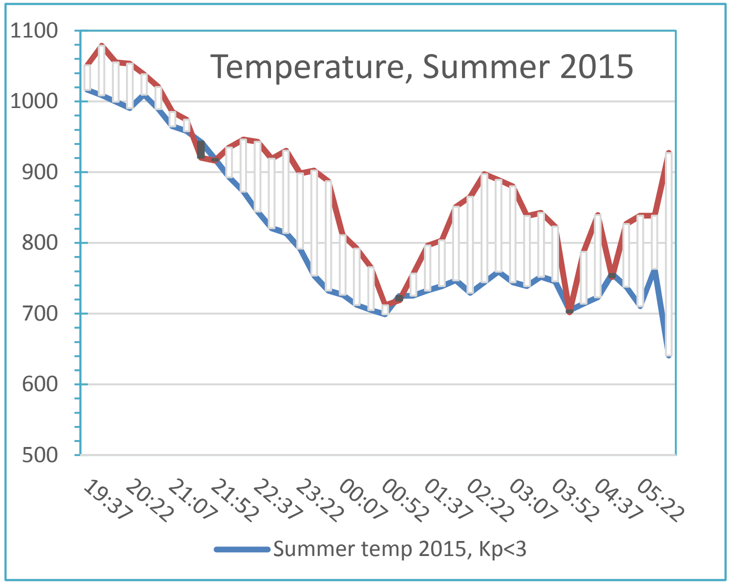

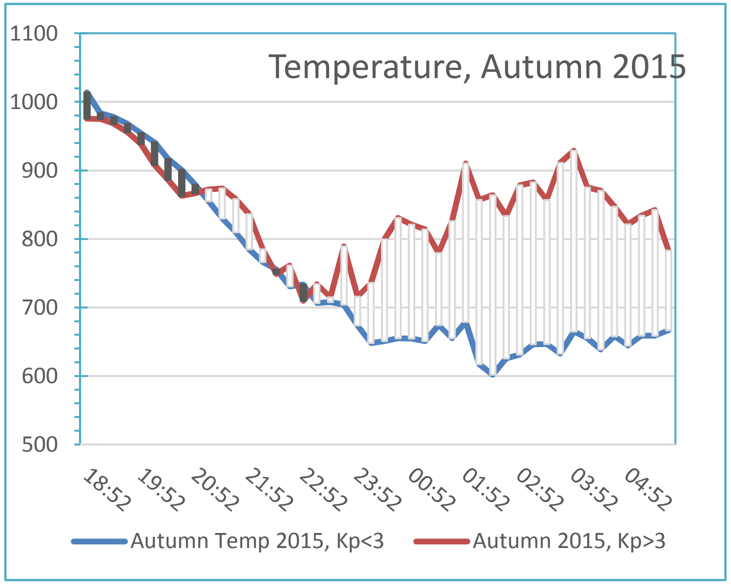

Case study of a geomagnetic stome; 27 February 2017

Sun and Interplanetary conditions

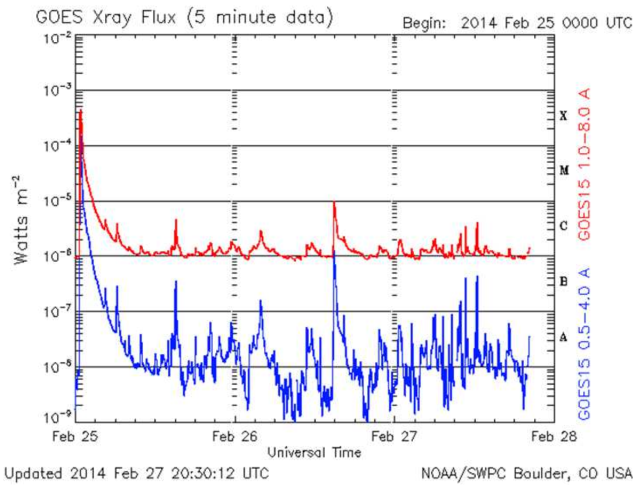

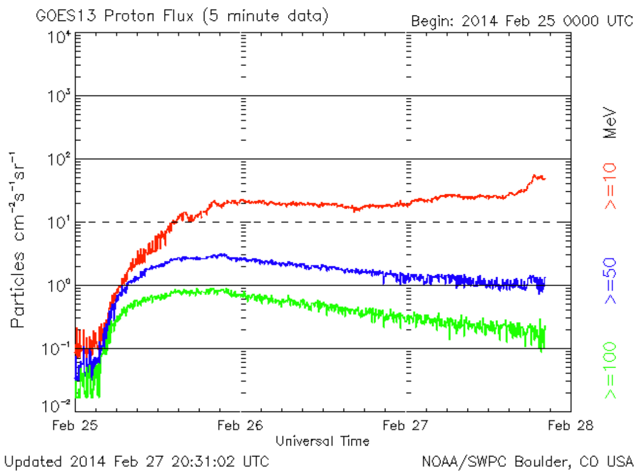

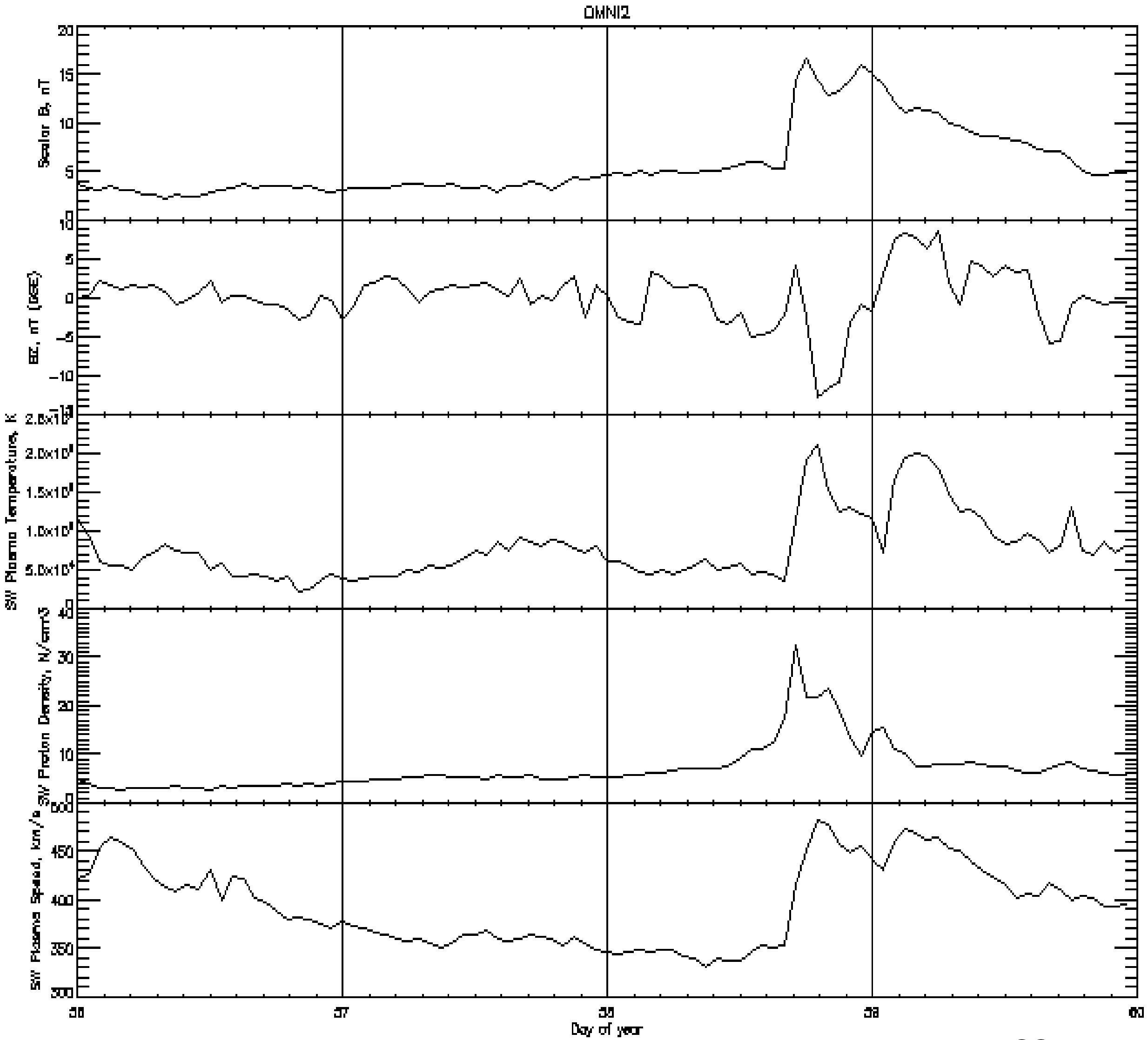

Storm time thermosphere-ionosphere coupling at midlatitude consecutive to an associated flare/CME event; a case study.

Geomagnetic indices

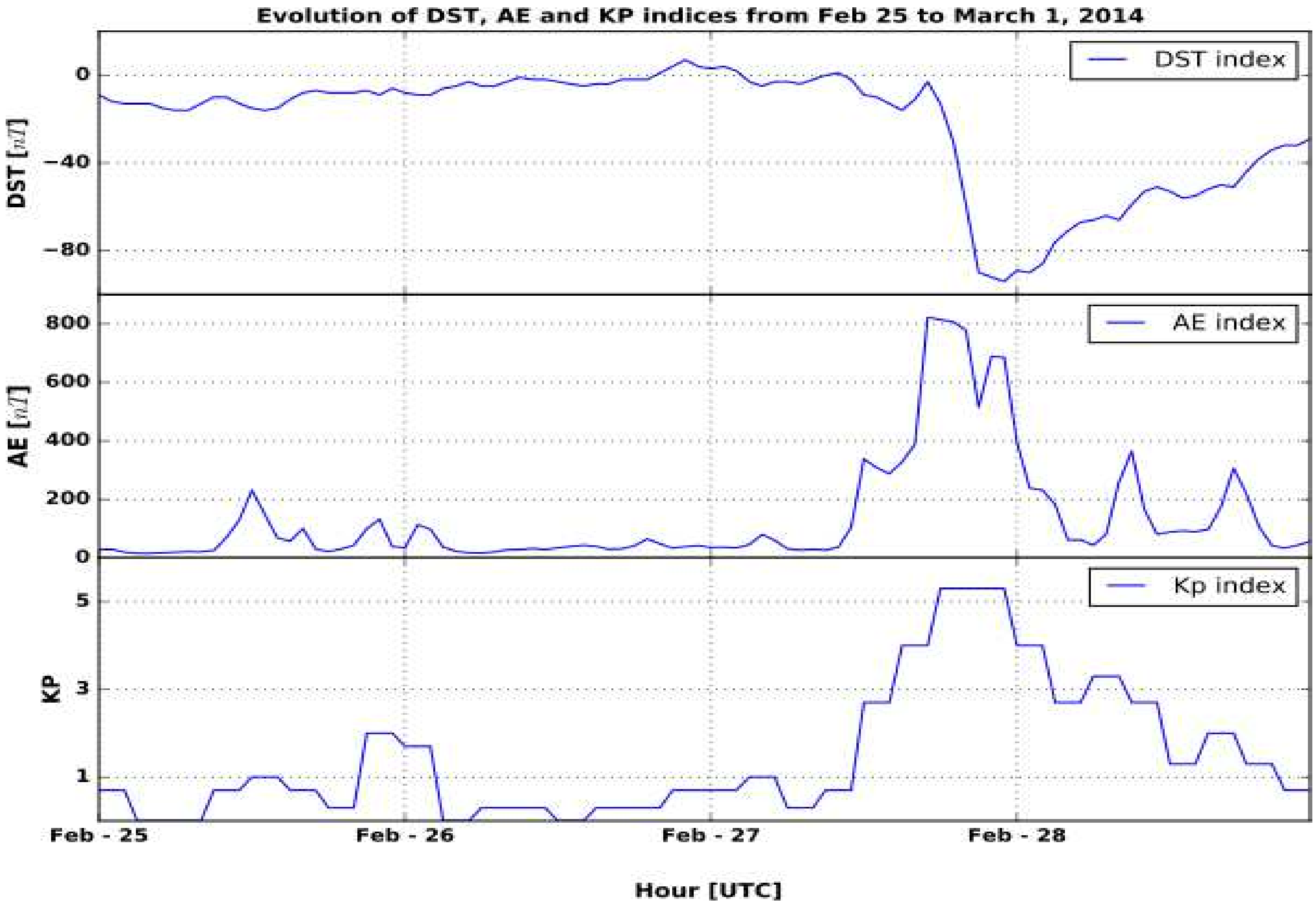

Storm time thermosphere-ionosphere coupling at midlatitude consecutive to an associated flare/CME event; 27 February 2014

Thermospheric wind response

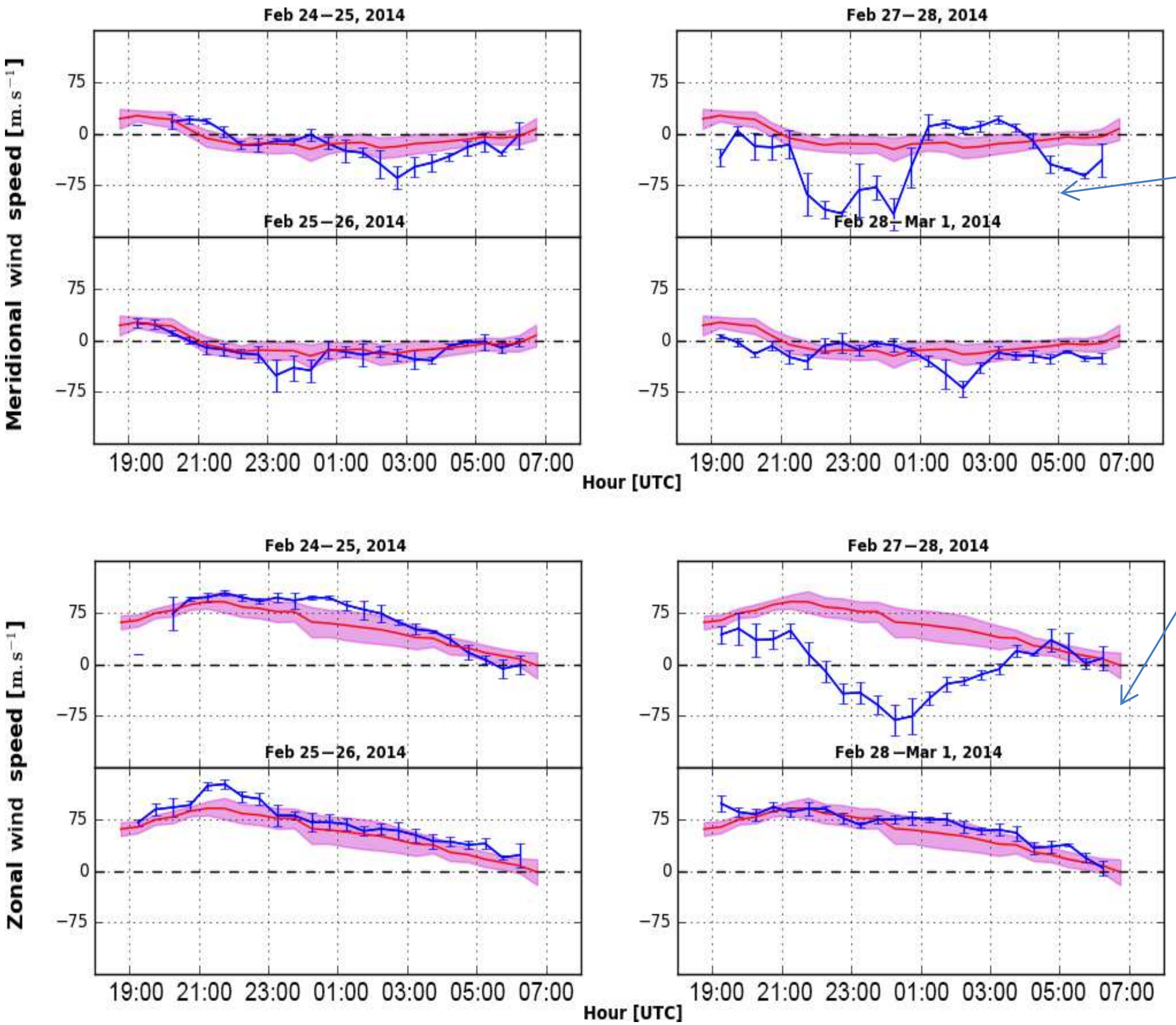

Departure fom climatological Behavior:

- Equatorward meridional winds. (140ms^{-1})
- Westward zonal winds (140ms^{-1}.)

Signature of thermospheric traveling atmospheric disturbances (TADs).

* First TAD Northward Captured around 21:00UT
* Second TAD coming from the Southern Hemisphere Captured around 00:00UT.

Storm time thermosphere-ionosphere coupling at midlatitude consecutive to an associated flare/CME event; 27 February 2014

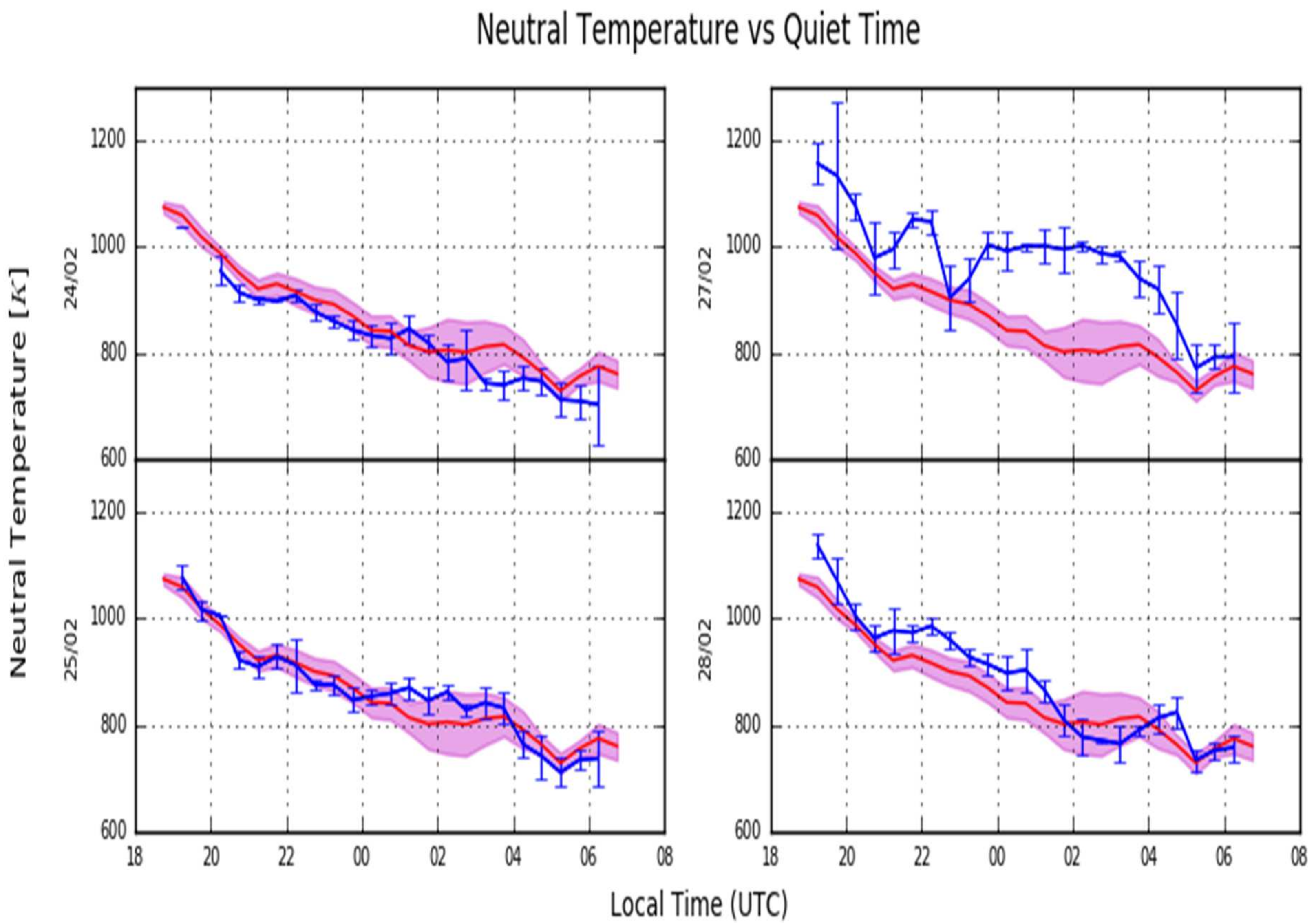

Storm time thermosphere-ionosphere coupling at midlatitude consecutive to an associated flare/CME event; 27 February 2014

Thermospheric wind response

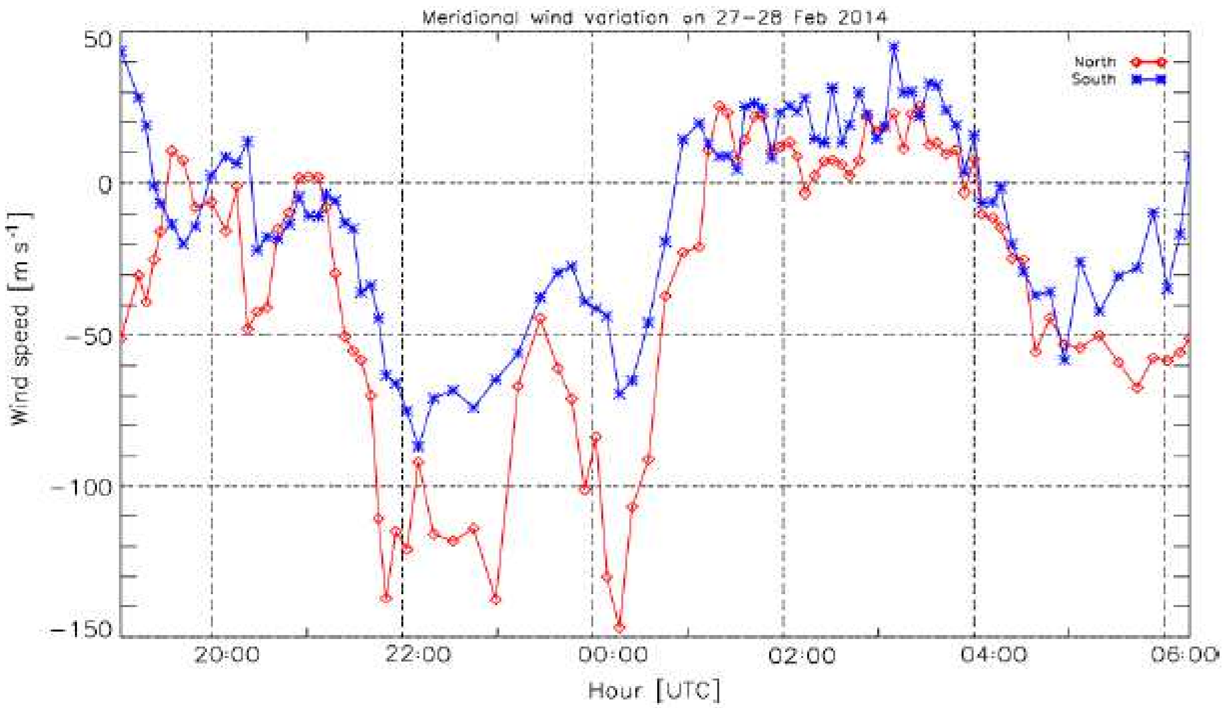

Clear view with the North and South Look direction of the meridional winds

wind gained a speed of almost 150 ms−1 in less than an hour.

↓

TAD

- First TAD coming from the northern hemisphere was captured around 21 LT, **lasted for about 4 hours**; (Vn > Vs) ΔT = 15 mn ------→ **V(TAD) = 550 m/s**

[Chao Xiong et al 2015] , [Sean L. Bruinsma and Jeffrey M. Forbes, 2007]

- Second TAD trans-equatorial was captured around 00 LT, **lasted for 3,5 hours**; (Vs > Vn)

Storm time thermosphere-ionosphere coupling at midlatitude consecutive to an associated flare/CME event; 27 February 2014

Thermospheric wind response

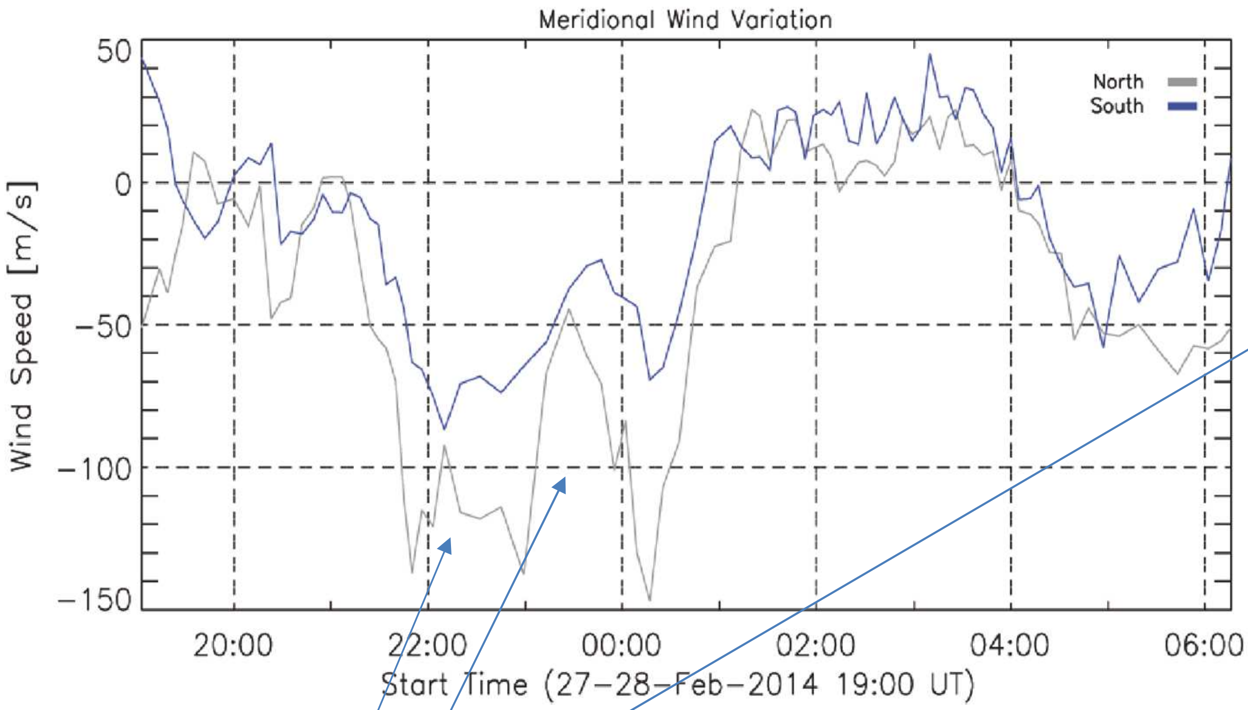

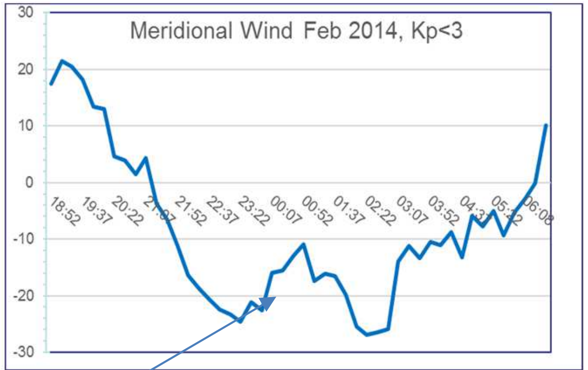

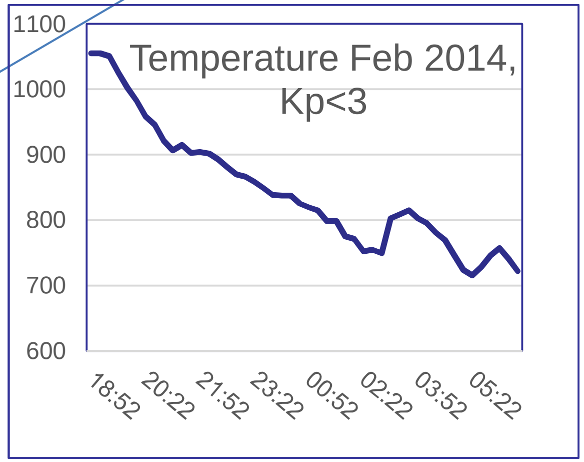

Reactive effects 1 and 2
Enhancement of the MTM phenomena due
To storm circulation (ΔV~100 m/s)

Midnight Temperature Maximum
MTM phenomena
Quiet time
(ΔV~20 m/s)

Storm time thermosphere-ionosphere coupling at midlatitude consecutive to an associated flare/CME event; 27 February 2014

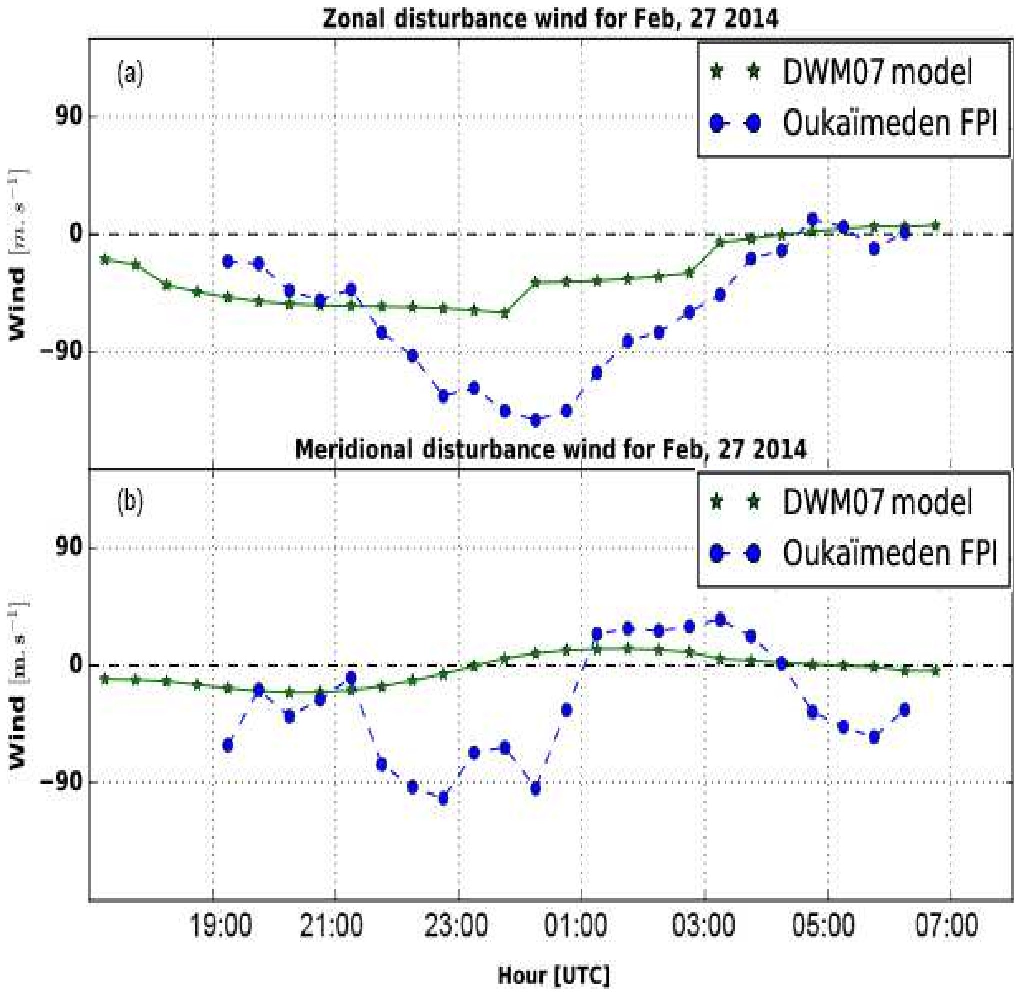

Thermospheric wind response, comparison with DWM07

Emmert et al. (2008) empirical wind model (DWM07)

The DWM07 model predictions provide a good indication of the new circulation pattern caused by storm activity, but it does not include the effects of TADs

Storm time thermosphere-ionosphere coupling at midlatitude consecutive to an associated flare/CME event; 27 February 2014

Steep decrease with ~ rate of 8,3 tecu/ hour.

Ionospheric electron density response

Rabat (33.99◦N; 353.14◦E, geographics)

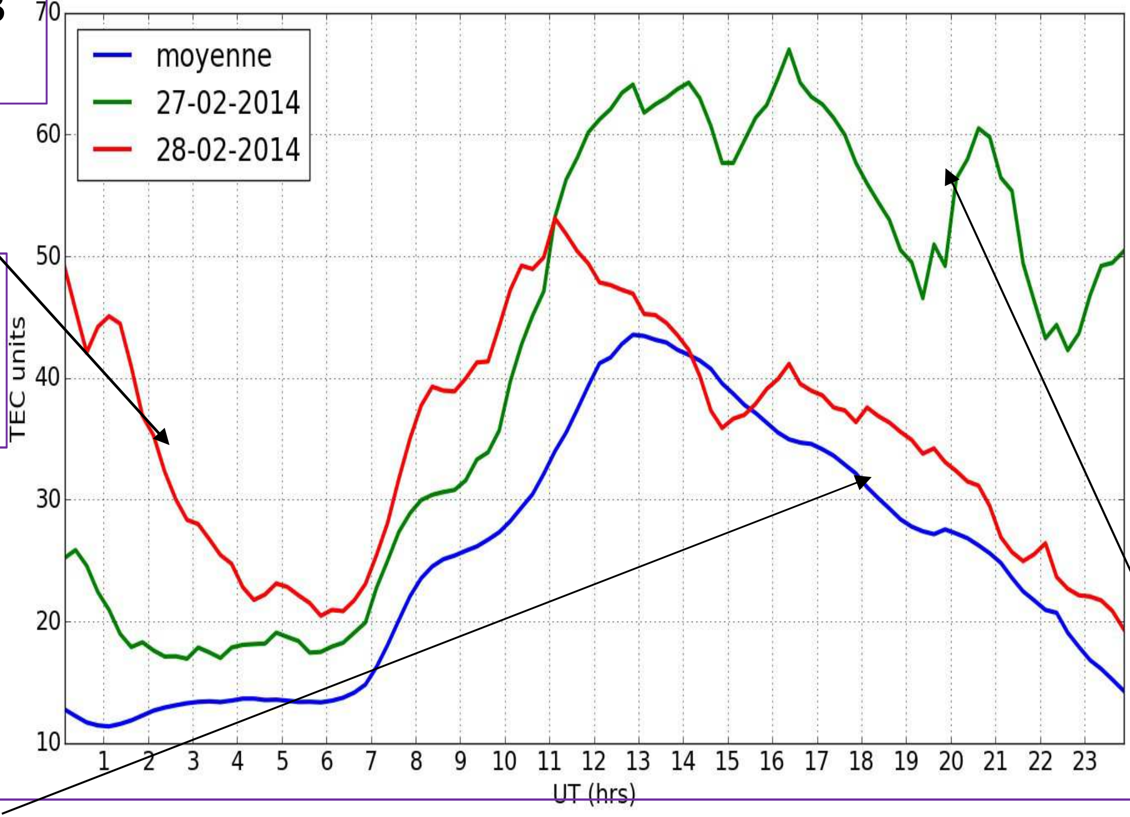

Positive storm consistent with (Fuller-Rowell et al., 1994, 1998).

Storm induced Traveling Ionospheric Disturbances **(TID)**

Quiet TEC

region (1) **from 07 to 13 UT,** TEC increases ~ linearly (rate =5 tecu/hour)
region (2) **from 13 to 00 UT,** TEC decreases ~ linearly (rate= 2,7 tecu/hour)
region (3) **from 00 to 07 UT,** TEC almost constant.

Storm time thermosphere-ionosphere coupling at midlatitude consecutive to an associated flare/CME event; 27 February 2014

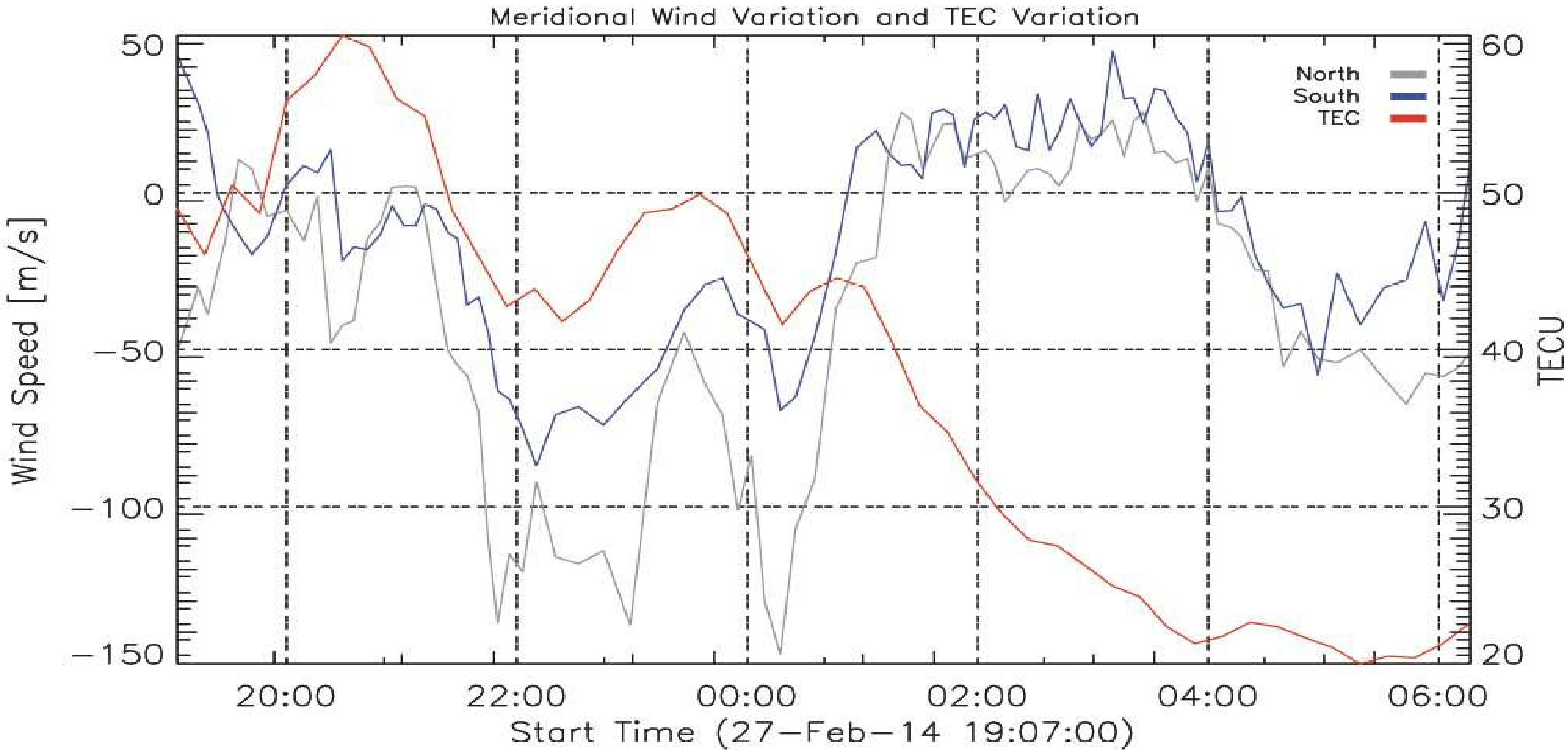

Between 19 and 00 UT, TEC correlates in some ways with the meridional winds.
Equatorward flow -----------→ decrease of the TEC.
Equatorward flow -----------→ raises the HmF2 pick where decrease NmF2 --------→ migration to thermospheric regions of increased mean molecular mass --------→ TAD effect.

Storm time thermosphere-ionosphere coupling at midlatitude consecutive to an associated flare/CME event; 27 February 2014

Electrodynamic response

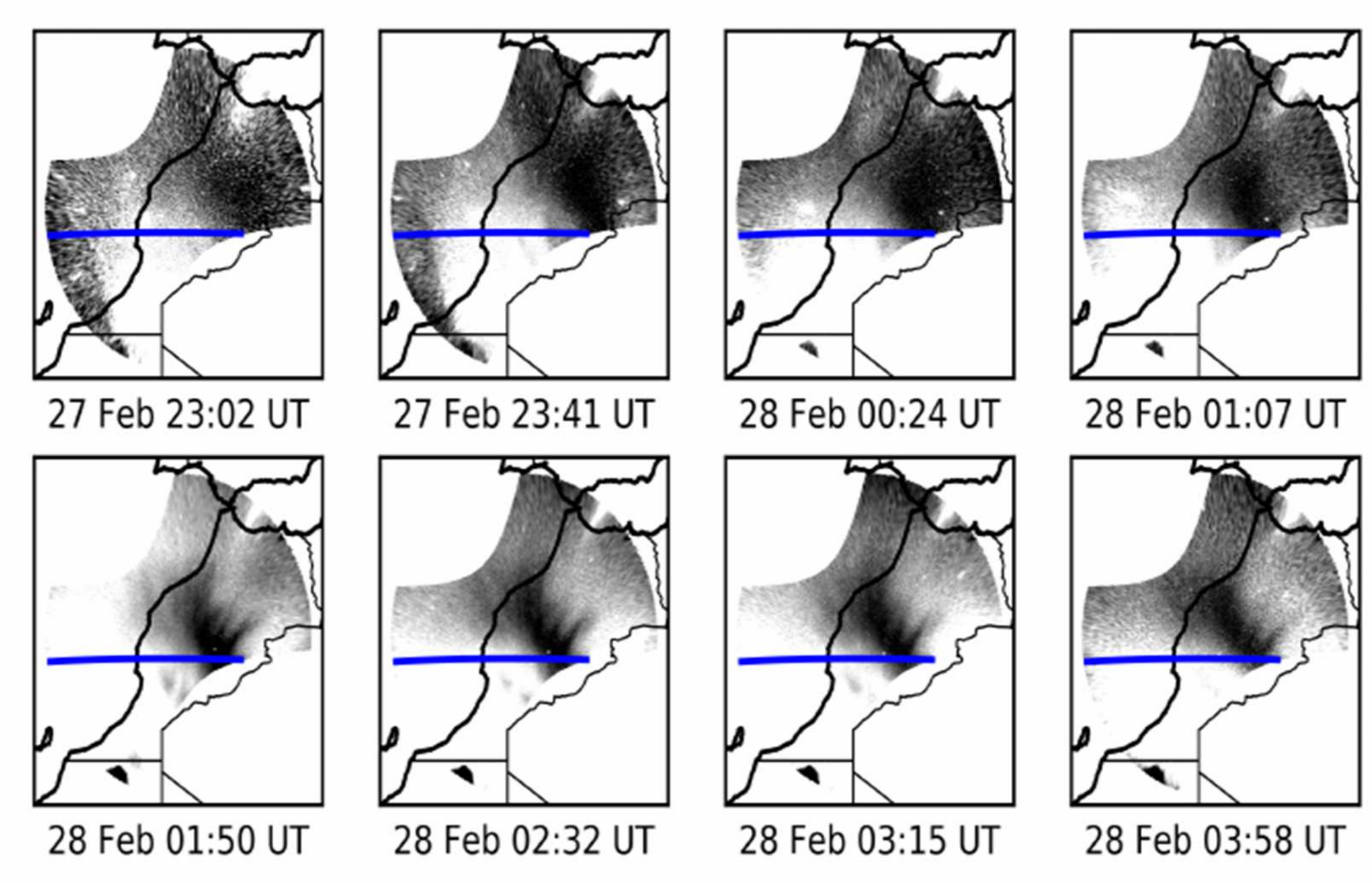

Eastward plasma bubbles motion until 22:00 UT, corresponding to the reversal of zonal winds.

Reversal of the background electric field direction as driven by the neutral wind disturbance dynamo

Storm time thermosphere-ionosphere coupling at midlatitude consecutive to an associated flare/CME event; 27 February 2014

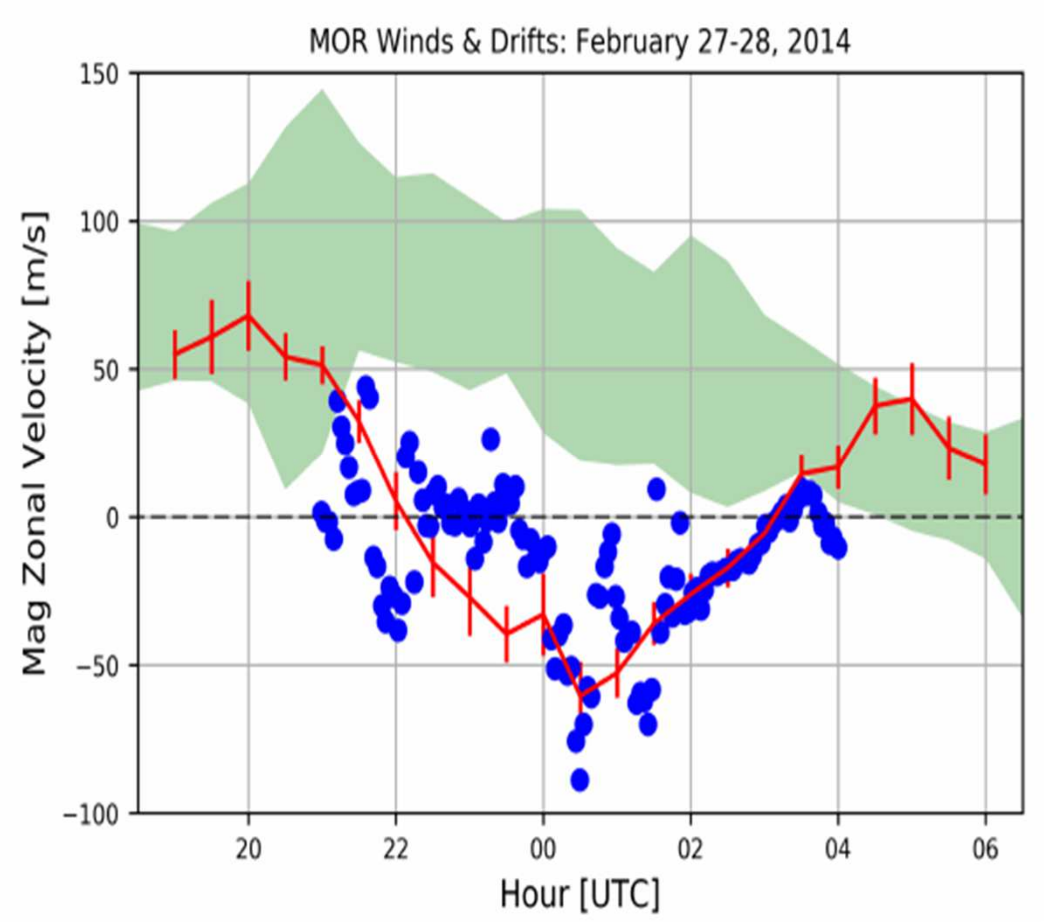

The plasma drift estimates from cross-correlations are marked as blue dots.

cross-correlation analysis

* Westward neutral winds, indicating forcing from the geomagnetic storm.

and

* EPB drifts tend to closely match the neutral winds

The dynamo is fully activated during this storm.

Storm time winds in general

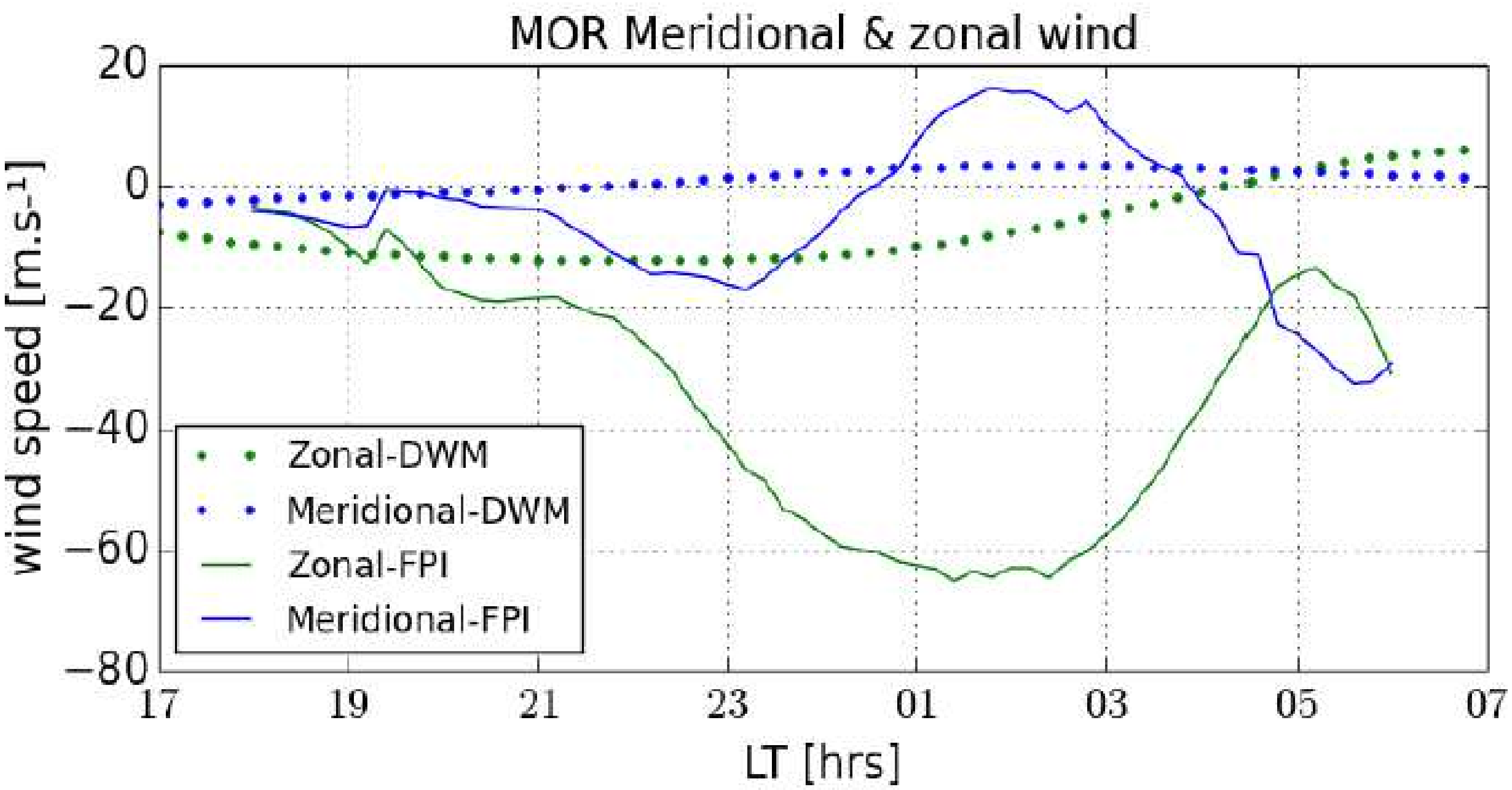

- 59 % of the cases are characterized by TAD induced circulation.
- 33 % exhibits only slight discrepancies between the disturbed and quiet night.
- 8 % are characterized by the transequatorial wind during the whole the night.

Storm time winds in general

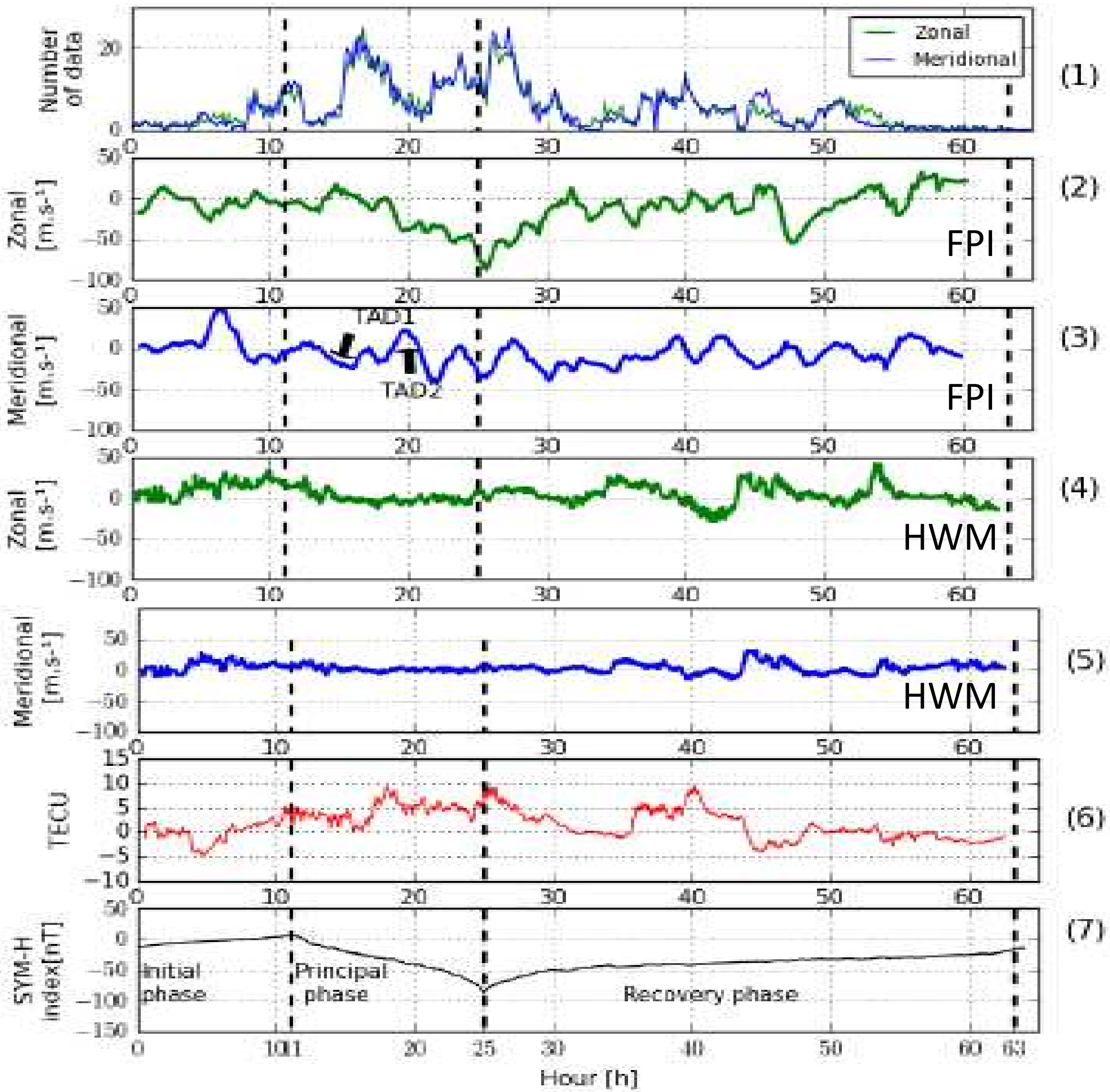

FPI observations and comparisons with thermospheric models: HWM14, NRLMSIS-00, TIE-GCM and GITM

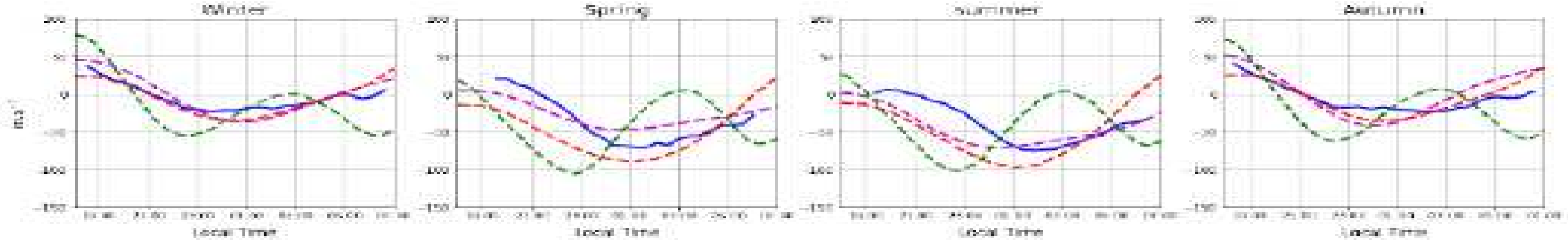

Figure 6. Seasonal comparison of meridional neutral winds between FPI-mesurememnt (bleu) and the HWM14(purple), TIE-GCM(red) and GITM (green) models predictions.

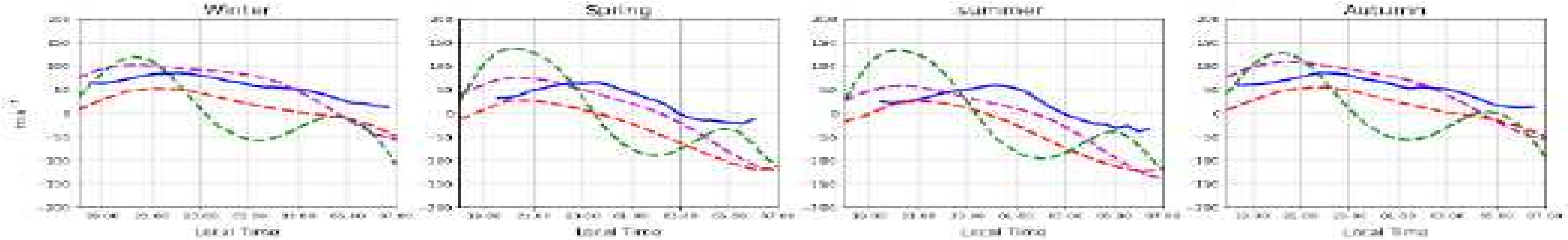

Figure 7. Seasonal comparison of zonal neutral winds between FPI-mesurememnt (bleu) and the HWM14(purple), TIE-GCM(red) and GITM (green) models predictions.

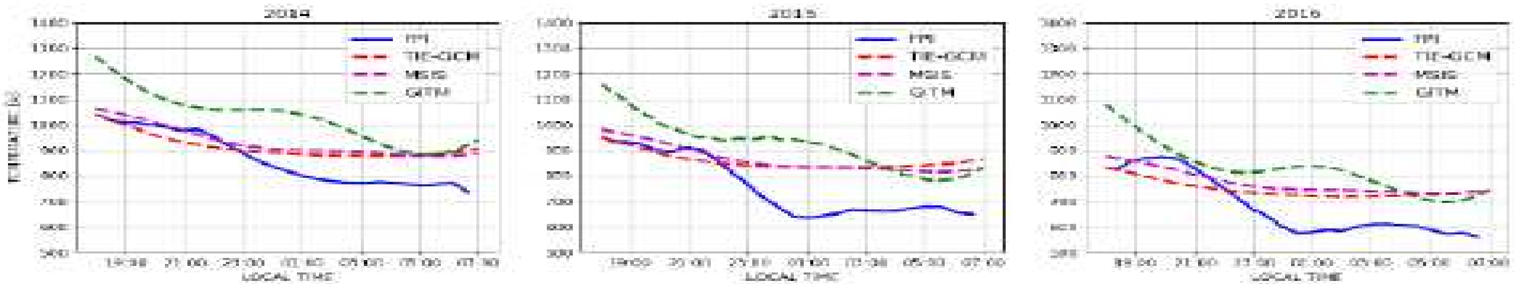

Figure 8. Yearly averages comparison of neutral temperature over three years 2014, 2015 and 2016 between Oukaimden FPI-measurements (bleu) and the simulations of NRLMSIS-00(purple), TIE-GCM(red) and GITM (green).

Longitudinal winds variability

Case study of two stations; Oukaimeden and Paris

	Geographic	Geomagnetic
PAR	35.2 N	45.27 N
MOR	31.21 N	22.73 N

Latitudinal and longitudinal winds variability

Meridional winds

- Poleward to equatorward reversal ~19-21 LT
- Maximum equatorward flow around local midnight
- Equatorward to poleward reversal ~03-05 LT
- Pattern shifts equatorward from local winter to local summer
    - Reversals presumably occur in sunlight before/after observations commence
- Generally consistent between MOR and PAR, although local winter equatorward winds appear suppressed over MOR

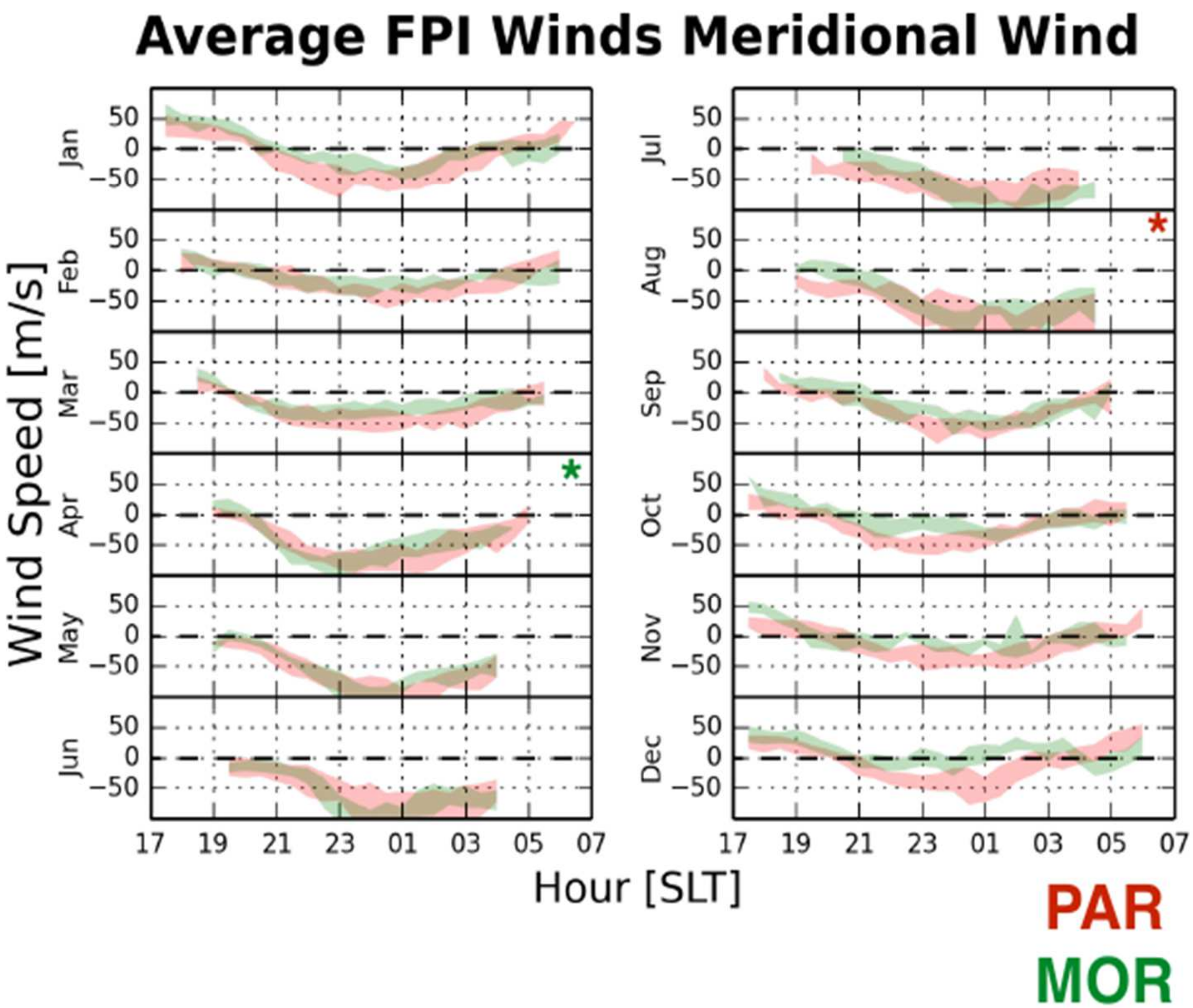

Longitudinal winds variability

Zonal winds

- Eastward to westward reversal occurs post midnight
  - Reversal occurs ~2 hours earlier over PAR than over MOR
  - Reversal time is a function of season (earlier in local summer)
- Stronger eastward flow over MOR than over PAR, especially during local summer
- Comparatively large phase shift seen over MOR in local summer

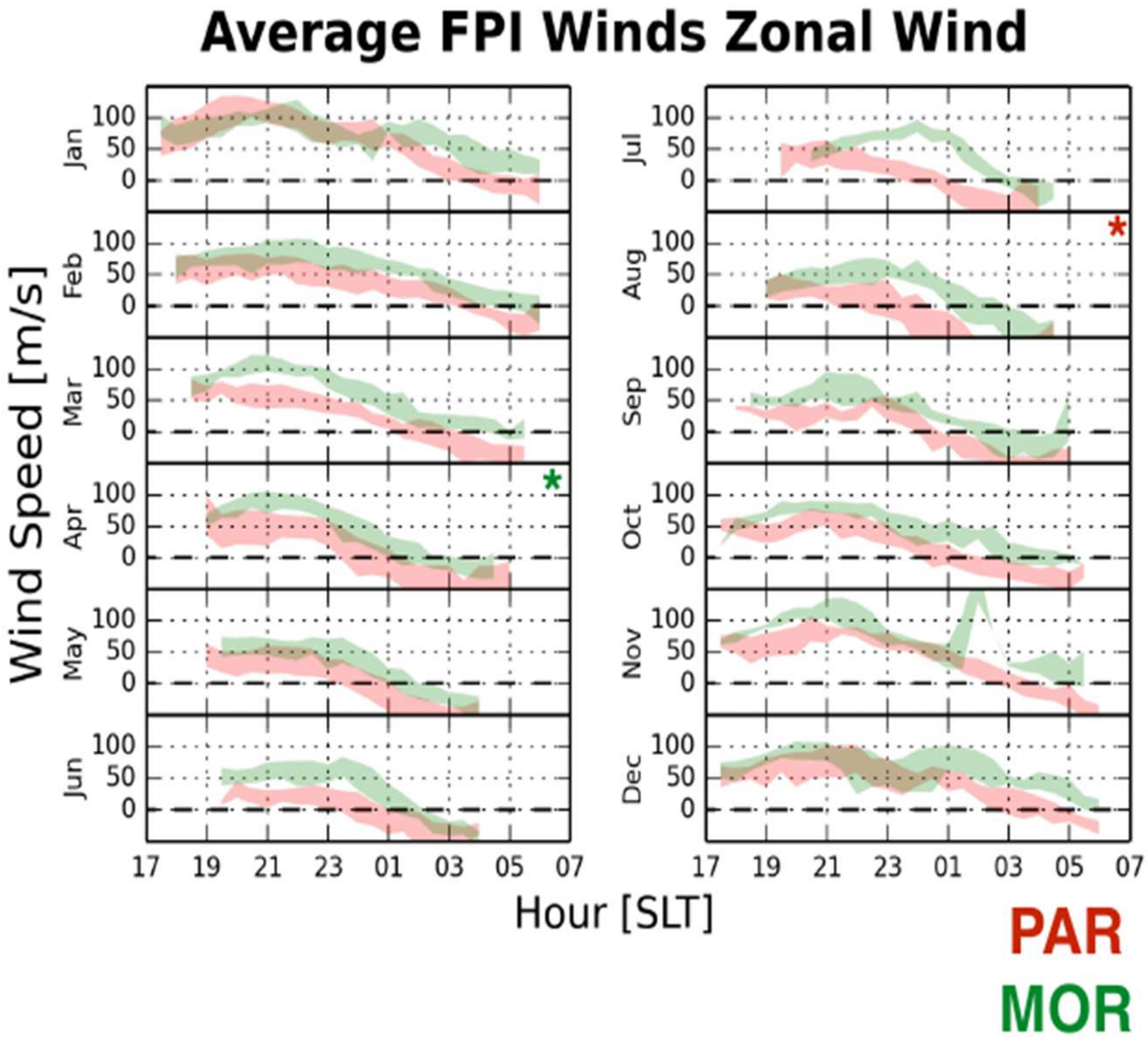

Longitudinal winds variability

Zonal wind from satellites

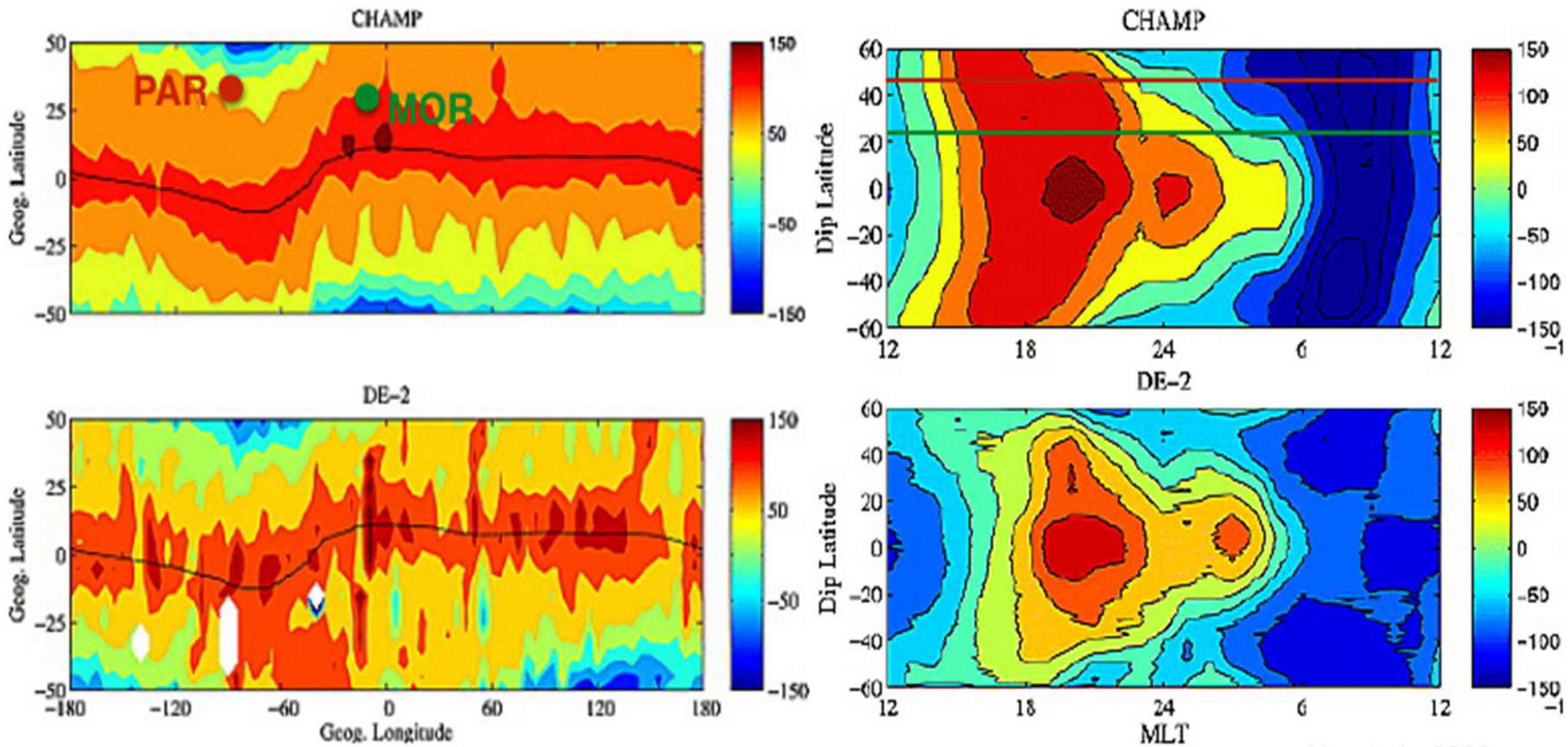

Liu et al., 2009

- Larger zonal wind over MOR is consistent with CHAMP/DE-2 measurements (averaged over 18-24 MLT)

- Progression of eastward-to-westward turning to later times as the magnetic equator is approached is also consistent between ground-based and satellite measurements (averaged over all seasons)

Stormtime response (Feb 28, 2014)

- Strong westward turning of winds over MOR during main phase of storm
    - Slight turning over PAR (during recovery)

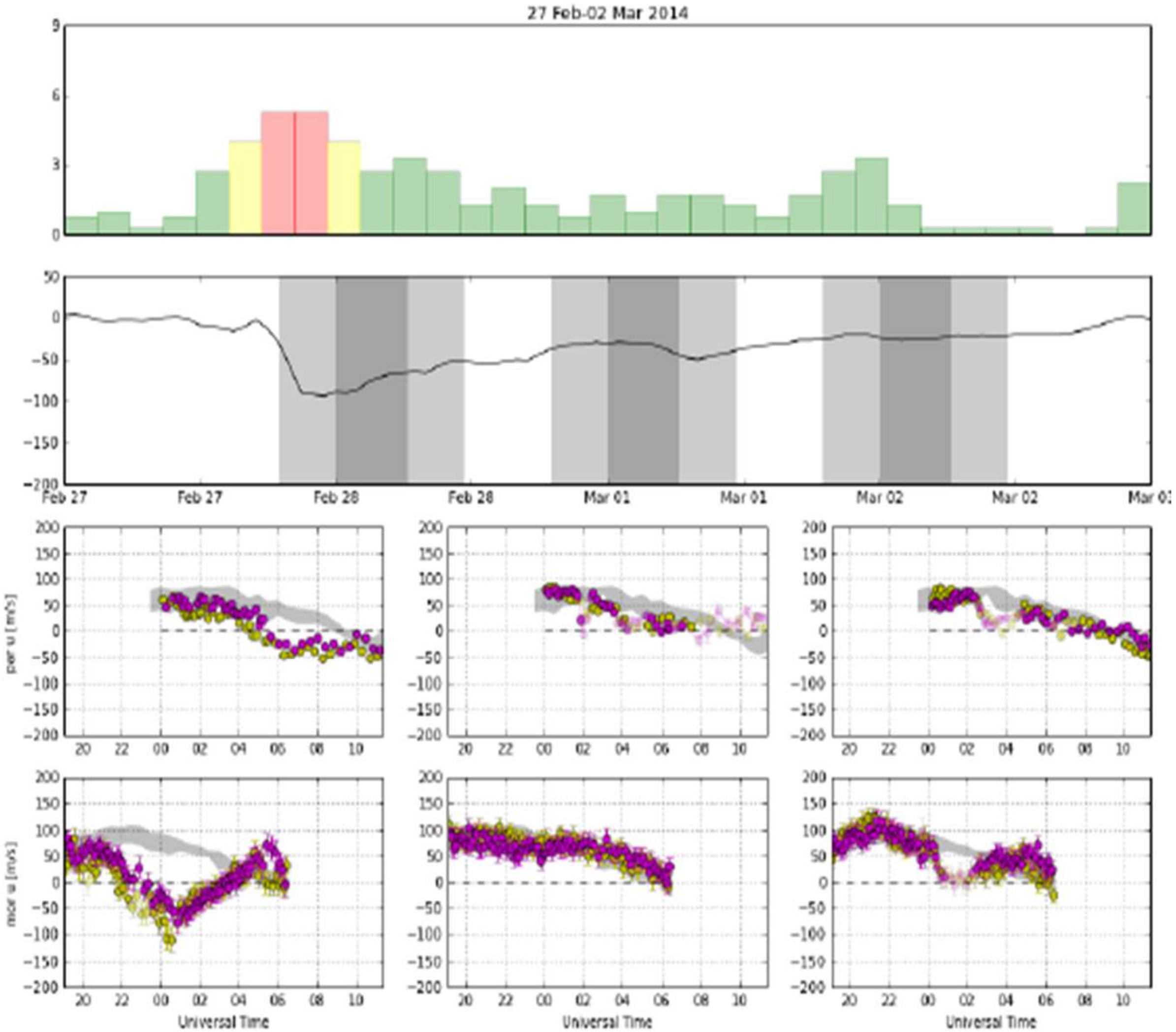

Stormtime response (Feb 28, 2014)

- Strong westward turning of winds over MOR during main phase of storm
    - Slight turning over PAR (during recovery)
- Enhanced equatorward winds over MOR, followed by a reversal to slightly poleward
    - Longer poleward duration over PAR

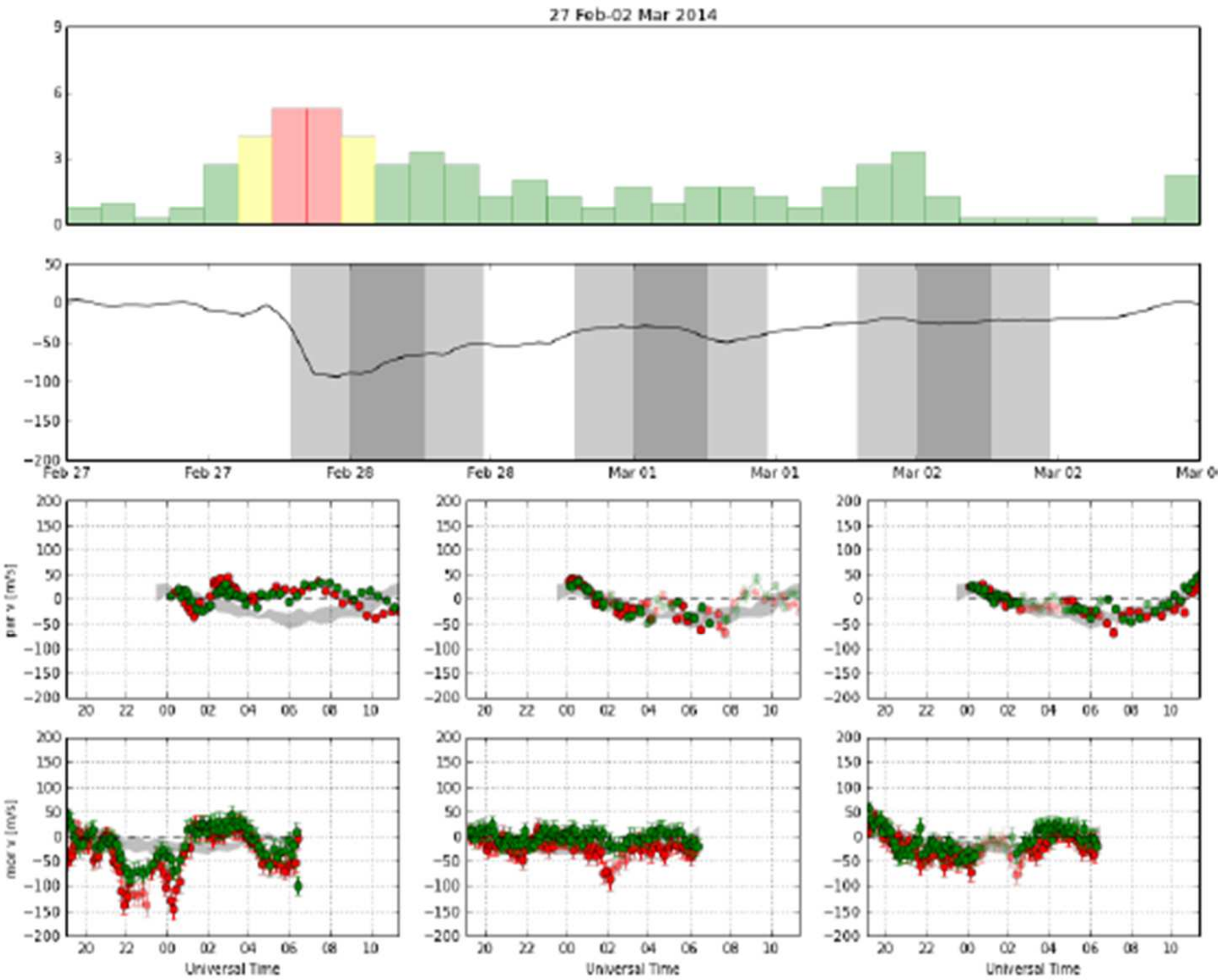

Stormtime response (June 23, 2015)

- Westward turning seen over both sites
  - Magnitude about 2x larger than seen in February 2014 (200 m/s vs. 100 m/s)

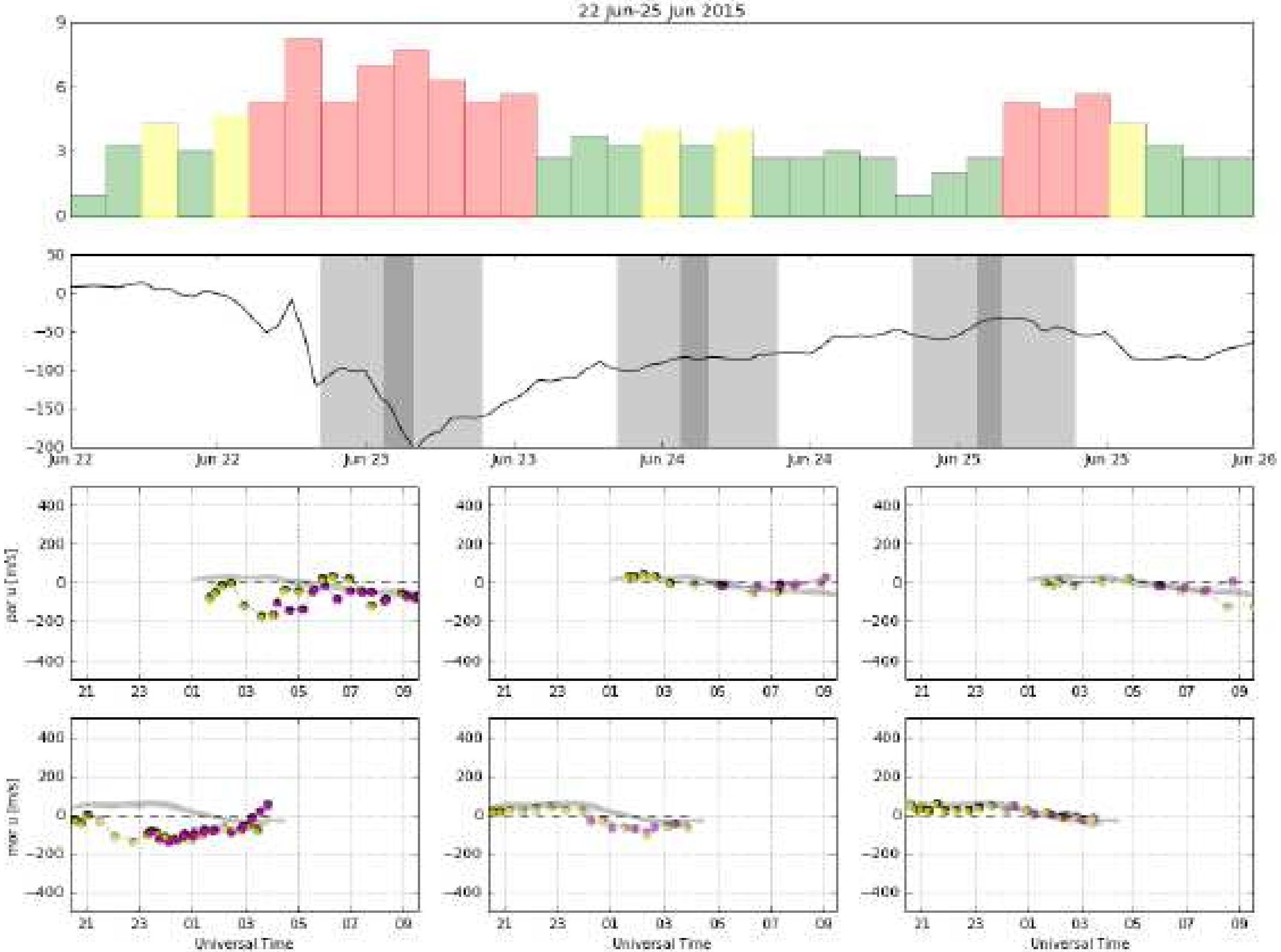

Stormtime response (June 23, 2015)

- Westward turning seen over both sites
    - Magnitude about 2x larger than seen in February 2014 (200 m/s vs. 100 m/s)
- Strong equatorward enhancement of meridional winds
    - Greater than 300 m/s over MOR in the early morning

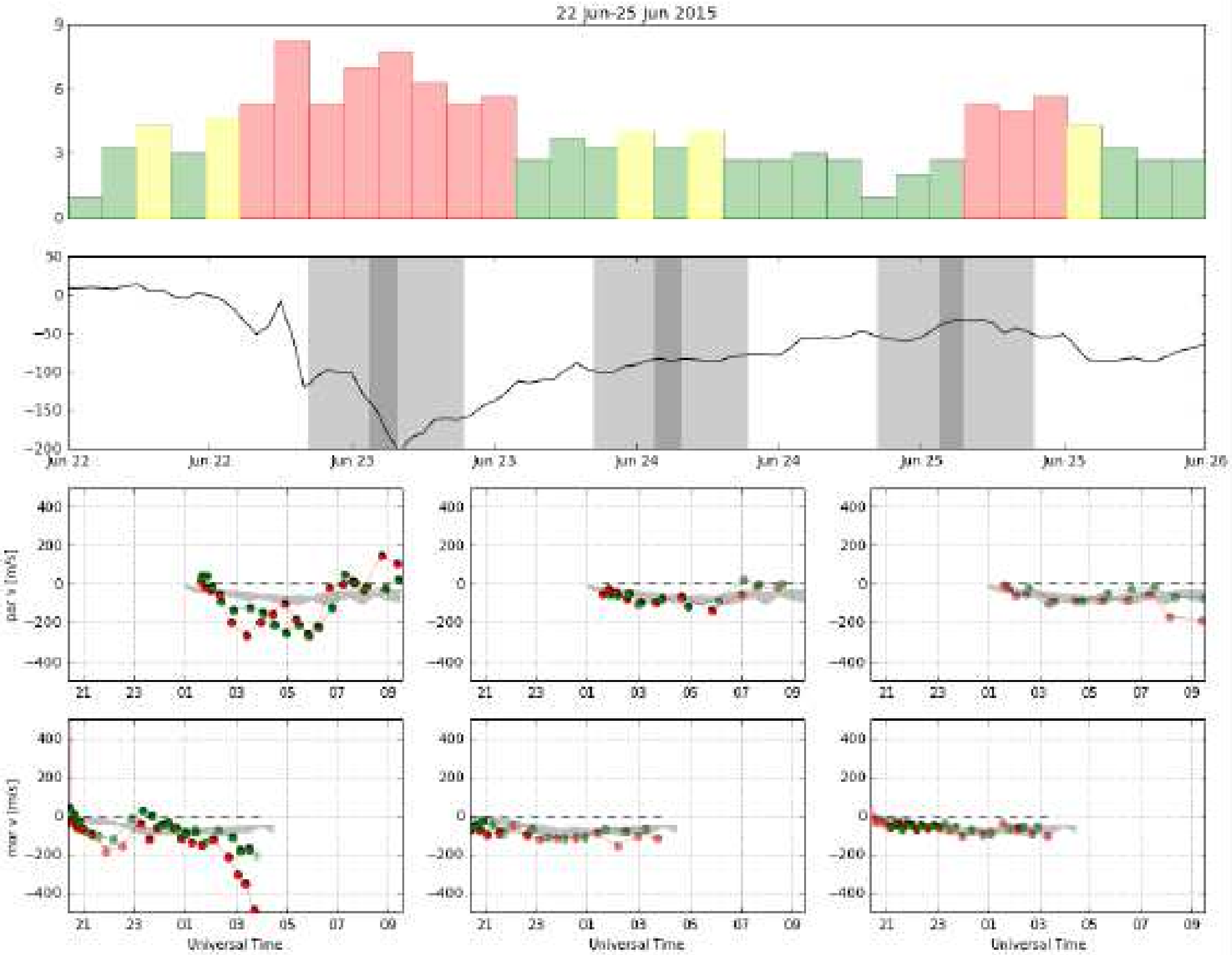

Interhemispheric asymmetry of the equatorial ionization anomaly (EIA)

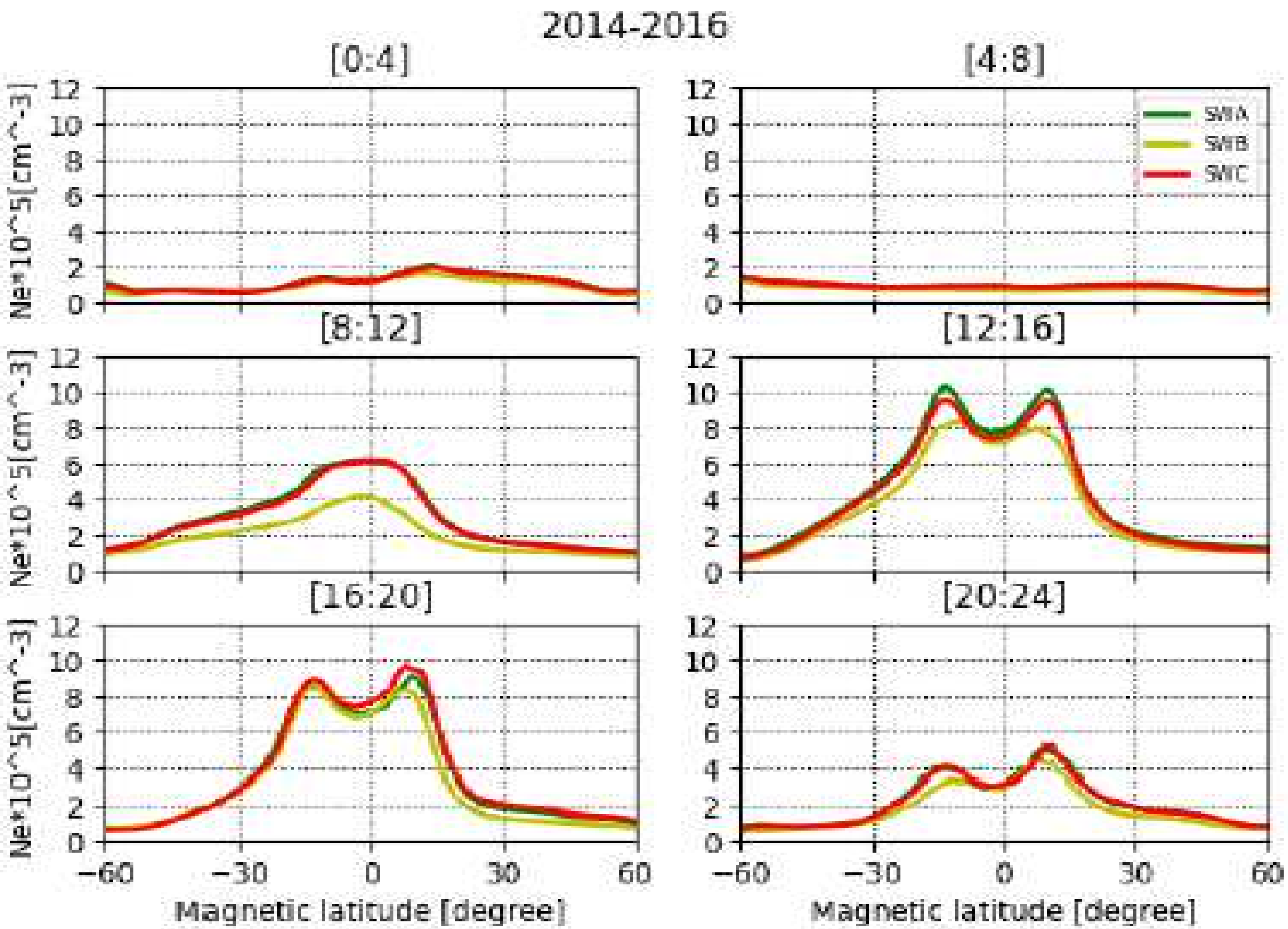

Average of three years of measurements

- From 24 to 8 LT, very low Ne.
- From 8 to 12 LT Ne increases with single crest.
- From 12 to 16 LT symmetric double crest.
- From 16 to 24 asymmetric double crest.

- The trend has in general clear asymmetry between north and south hemisphere.

Interhemispheric asymmetry of the equatorial ionization anomaly (EIA)

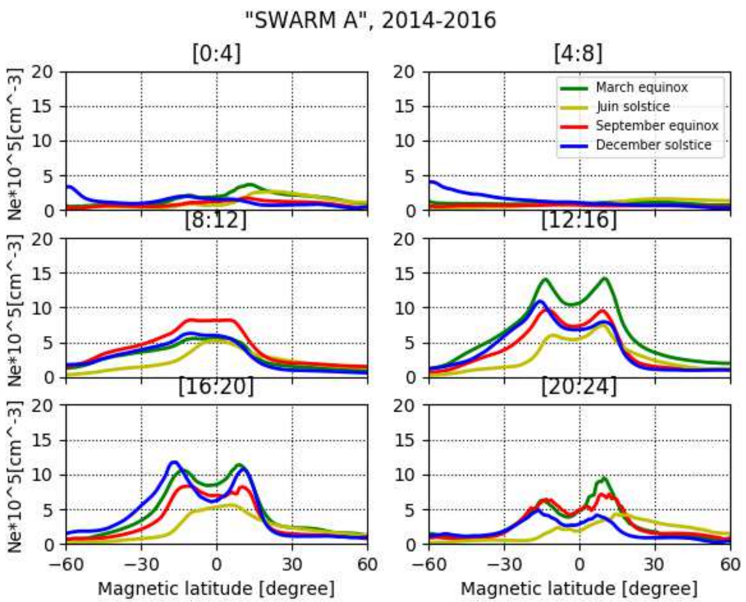

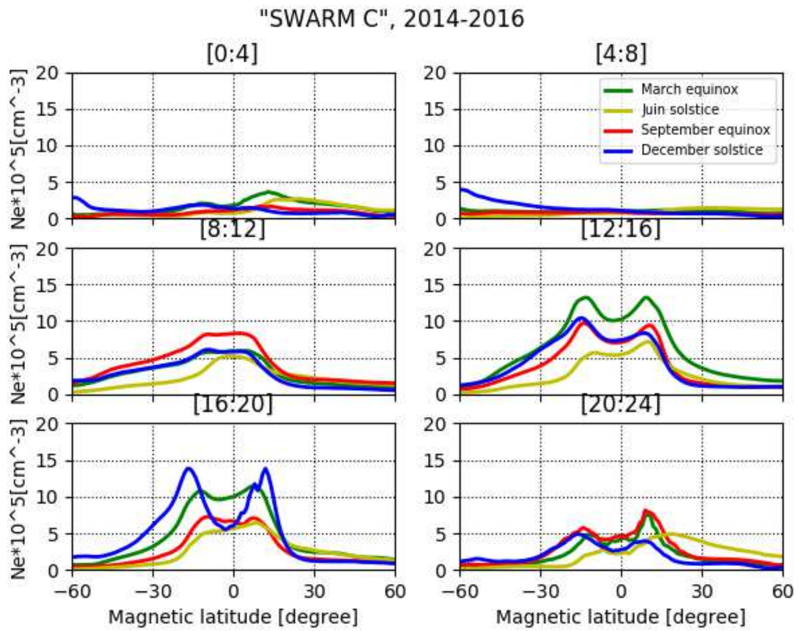

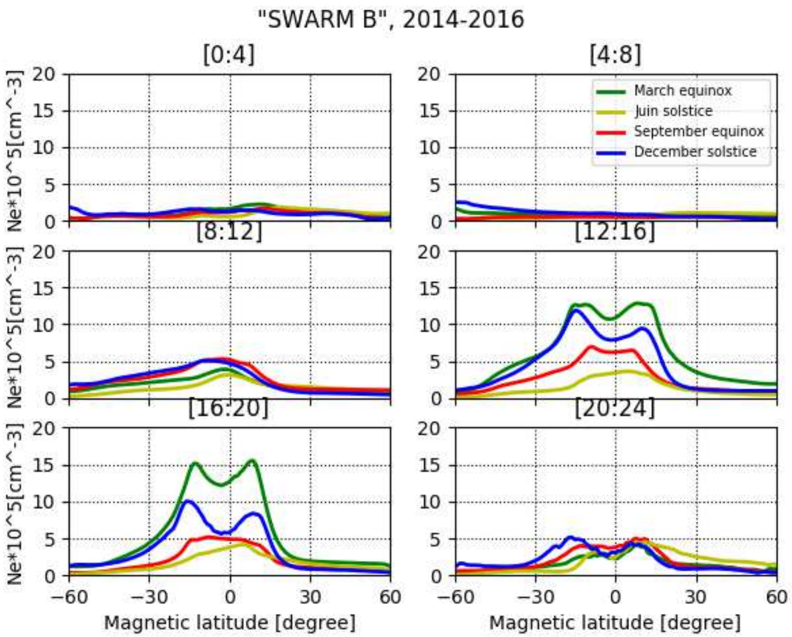

* June solstice, Ne is the lowest.
* Ne is higher around equinox than solstice : Semi-annual anomaly.
* For solstice seasons, the asymmetries in Ne are stronger at the December solstice than at the June solstice.
* Equinoctial symmetry.

* SWB, high Ne at 16-20 LT ?? Why ?

Effect of meridional neutral winds on equatorial ionization anomaly (EIA)

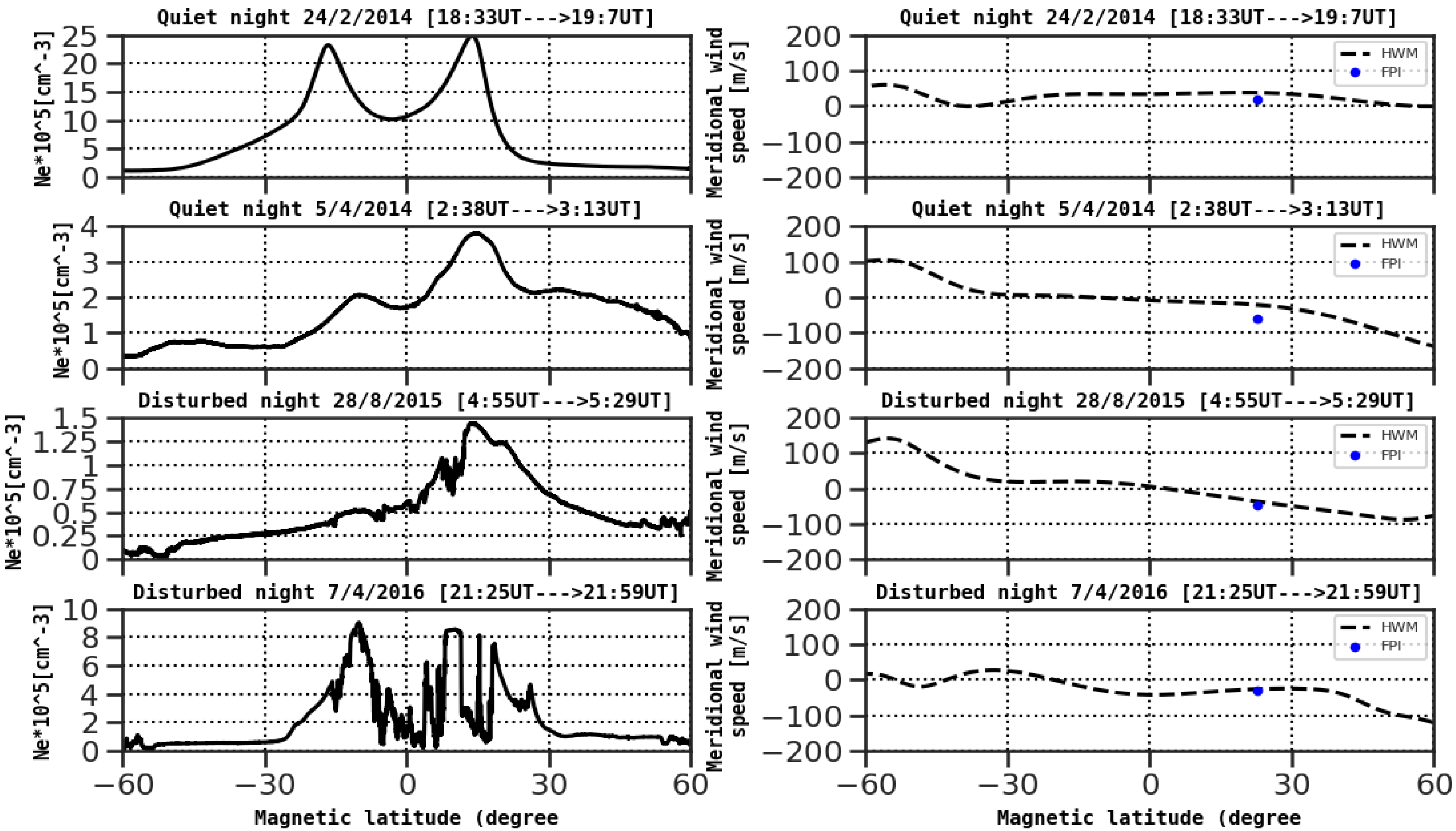

* Symmetrical EIA crests most likely is generated by either weak wind speeds or by converging/diverging winds with about the same velocity in both hemispheres.

* EIA crests asymmetry is observed along with transequatorial winds

Thermospheric winds over Africa

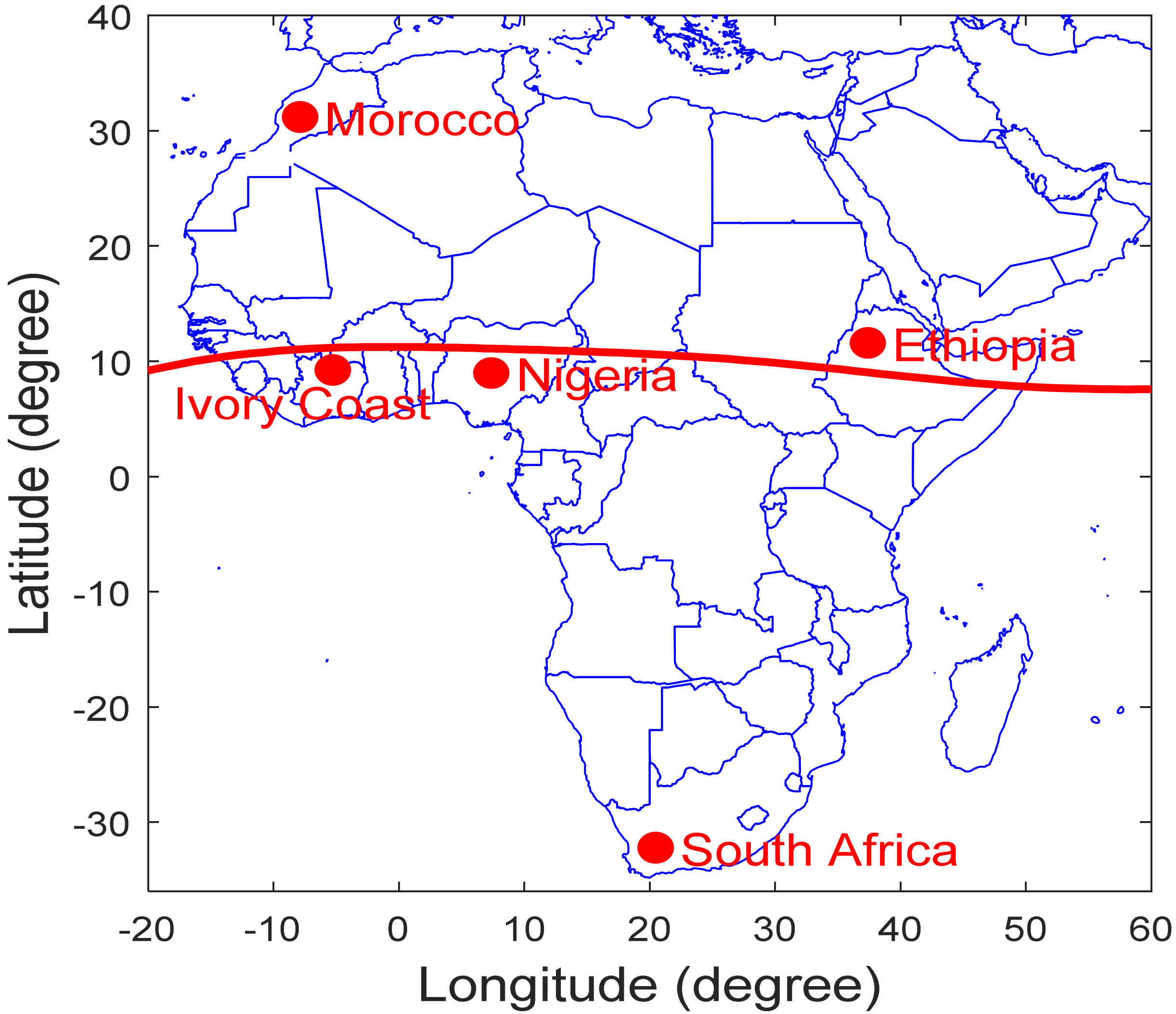

Thermospheric winds over Africa

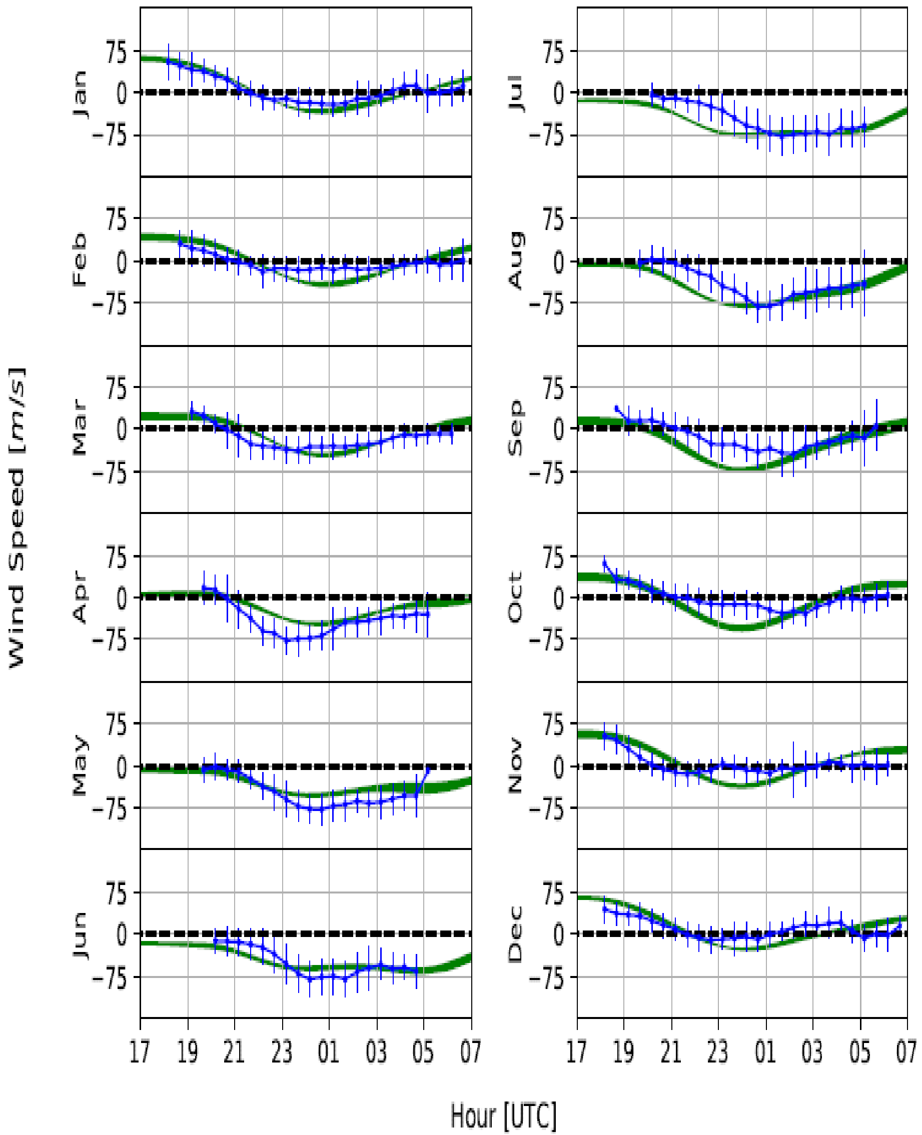

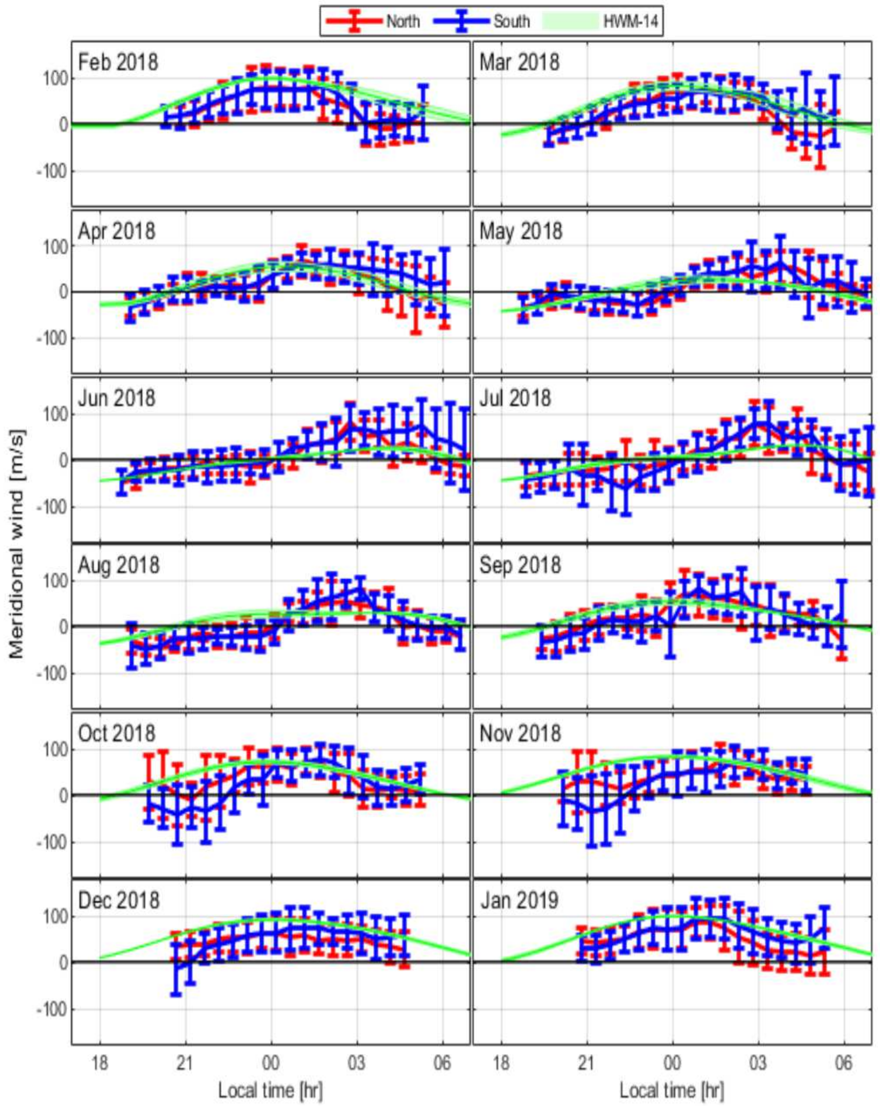

Oukaimeden; Geographic: 31.2ºN, 7.87ºW
Geomagnetic: 22.84ºN
Jan. 2014 to Feb. 2016

South Africa; Geographic: 32.2ºS, 20.48ºE
Geomagnetic: 40.7ºS
Feb. 2018 to Jan. 2019

Thermospheric winds over Africa

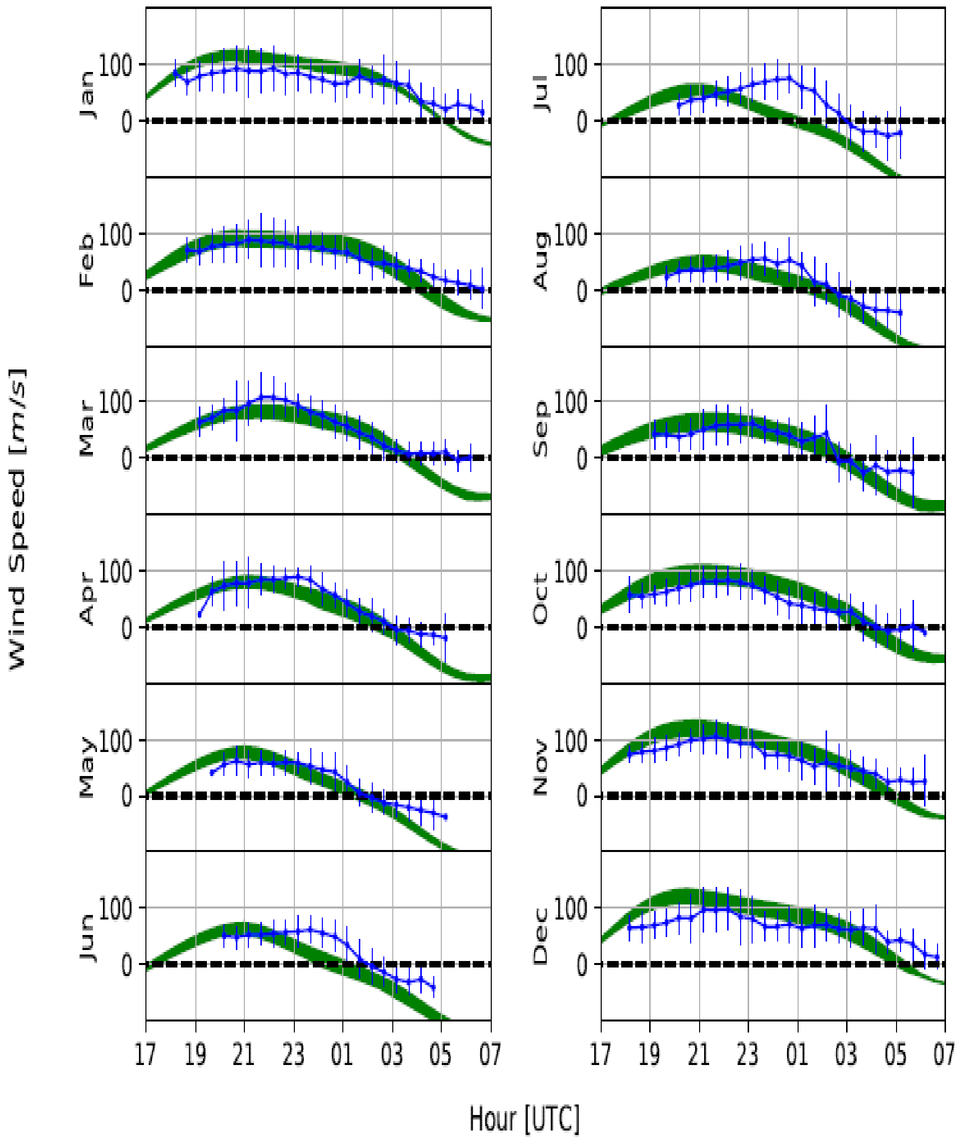

Oukaimeden; Geographic: 31.2°N, 7.87°W
Geomagnetic: 22.84°N

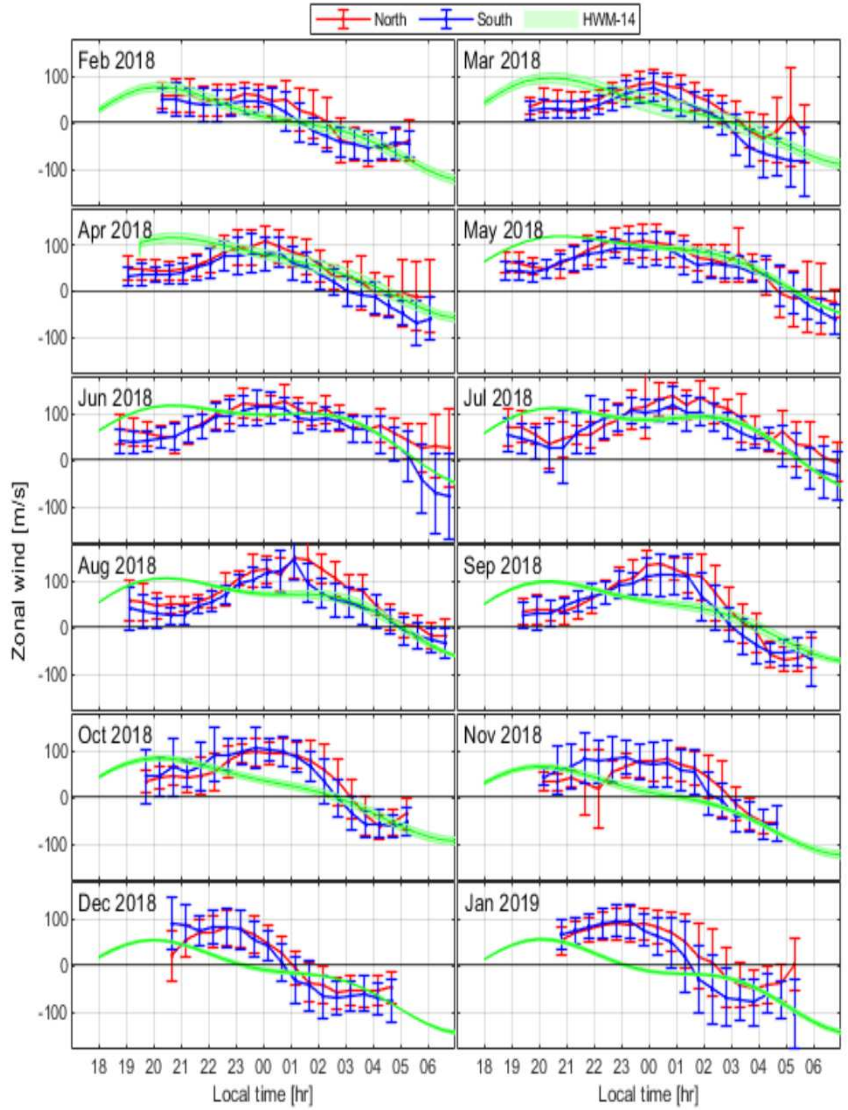

South Africa; Geographic: 32.2°S, 20.48°E
Geomagnetic: 40.7°S

Thermospheric winds over Africa

Ethyopia ; 11.6 N, 37.4 E, 3.7 N magnetic).

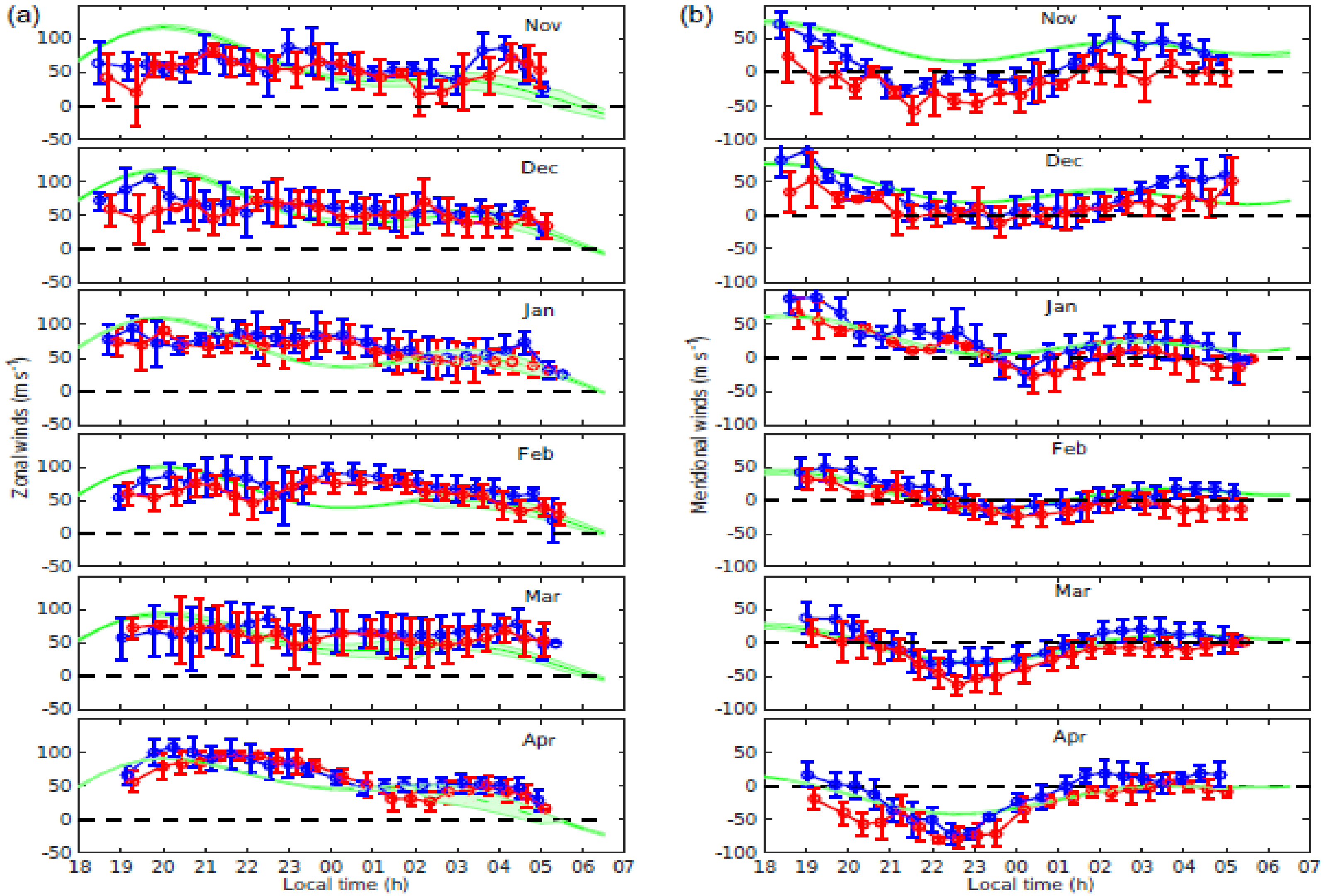

Zonal wind east (blue) and west (red) directions. Meridional wind; north (blue) and south (red) directions

Nov. 2015 to Apr. 2016

Thermospheric winds over Africa

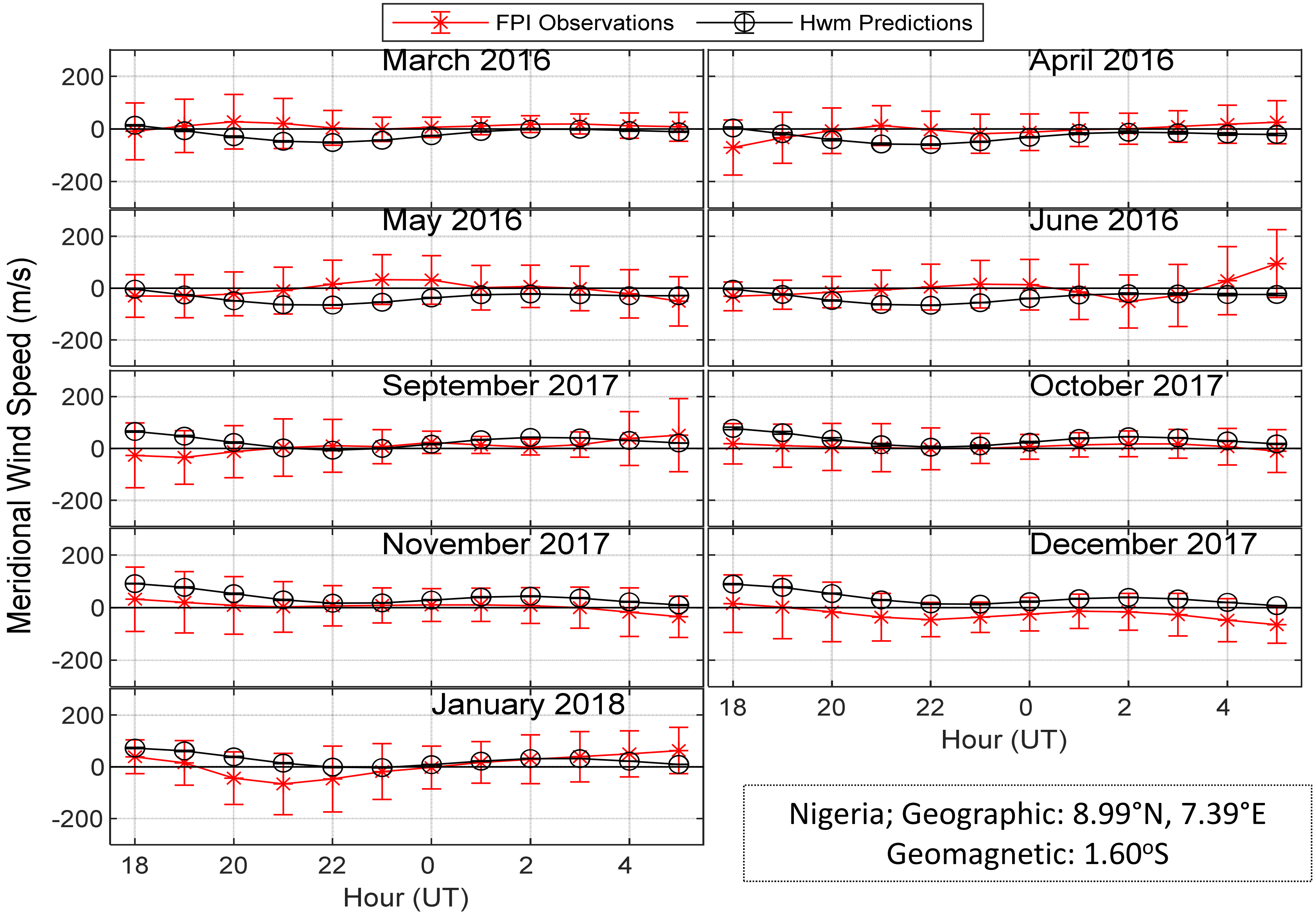

Nigeria; Geographic: 8.99°N, 7.39°E
Geomagnetic: 1.60ºS

Meridional winds in Nigeria for March 2016 to January 2018

Thermospheric winds over Africa

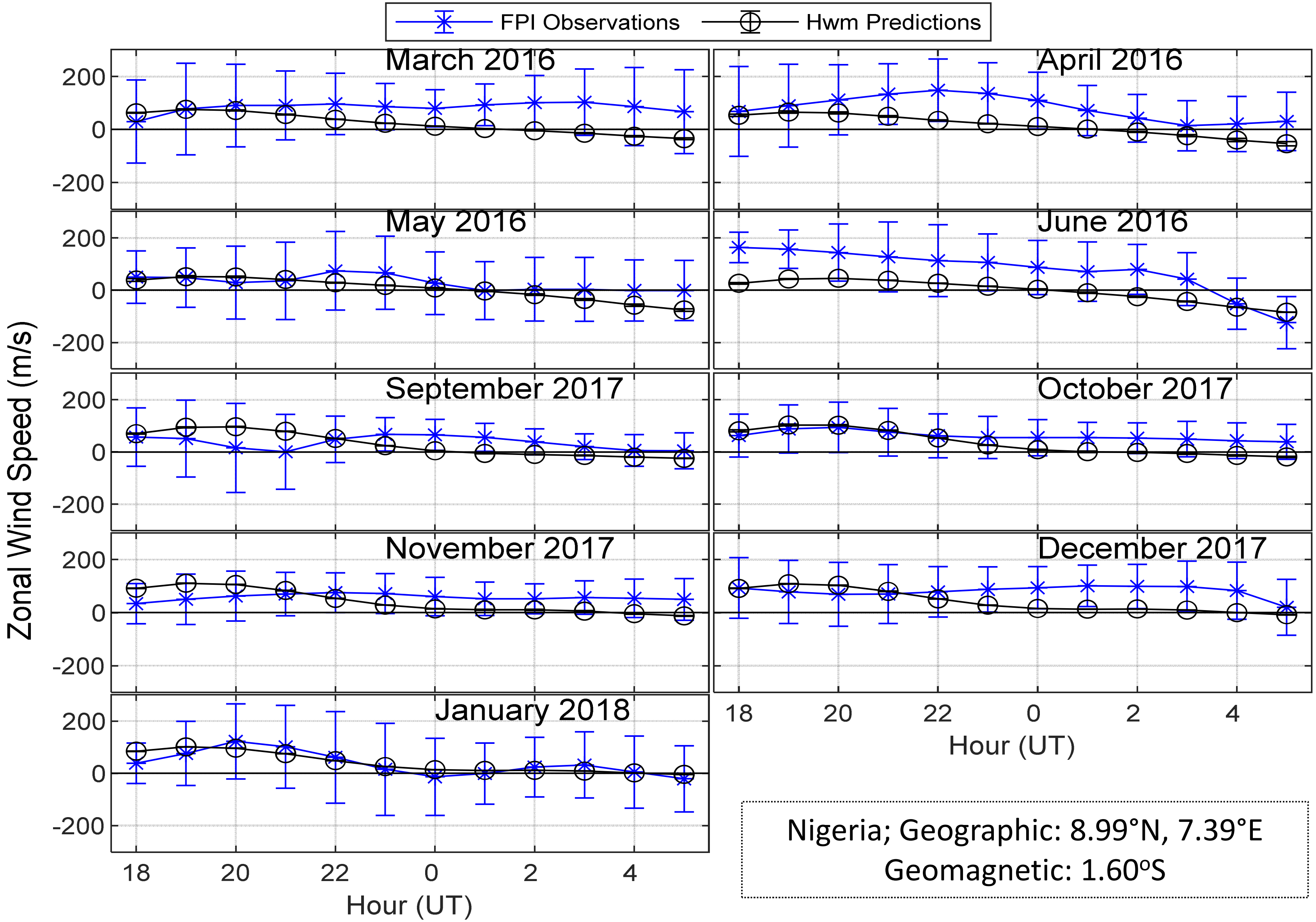

Nigeria; Geographic: 8.99°N, 7.39°E
Geomagnetic: 1.60°S

Zonal winds in Nigeria for March 2016 to January 2018

Thank you for your attention